

12. Radiation Damage

12. Radiation Damage	1
12.1 Introduction	2
12.2 Particle-Solid Interactions	2
Fig. 12.1: The interaction of particles with atoms in the solid	4
12.2.1 Cross section	4
12.3. Primary Knock on Atom (PKA) Energy Loss Mechanisms	6
12.3.1 Binary Elastic Collision Dynamics	8
Example #1 Energy transfer from neutrons to Fe-C	10
12.3.2. The limit between nuclear and electronic stopping	10
12.3.3. Electronic Stopping: energy transfer rate	11
12.3.4. Nuclear stopping	13
12.3.5 . Ion-Atom Scattering; General Binary Collision Dynamics	14
<i>Conservation of Energy</i>	15
<i>Conservation of Angular Momentum</i>	16
<i>Relation of Impact parameter to Differential cross section</i>	18
Example # 2 Rutherford Cross Section	18
12.4. The Displacement Process	20
12.4.1. Threshold Displacement Energy	20
12.4.2. Displacement Cascade and the Final Damage structure	22
Displacements within the cascade	24
12.5 Displacements per PKA	24
<i>The Kinchin Pease (KP) Model</i>	25
<i>Lindhard Scharff Schiott (LSS) Energy Partition Model</i>	26
<i>The Norgett-Robinson-Torrens (NRT) Model</i>	27
12.6. Displacements per atom caused by Neutron Irradiation	29
Example #3 Displacements in steel	31
Example # 4 Displacement rate in a fusion reactor first wall.	31
<i>Displacements calculated with the NRT model</i>	33
12.7. Other Measures of Radiation Damage	33
12.8 Other Displacement Mechanisms	35
12.8.1. Gamma Displacement damage	35
12.8.2. Thermal Neutron Reactions	39
Example # 5 displacements due to neutron activation of iron	39
12.8.3 Inelastic Scattering	40
Example # 6 Displacements from inelastic scattering of neutrons from iron	41
12.9. Charged-particle irradiation	41
12.9.1 Electron Irradiation	42
12.9.2. Ion Irradiation	43
12.9.3 TRIM and SRIM codes	45
Problems	47
References	52

12.1 Introduction

While in service, reactor materials are exposed to intense fast neutron and gamma fluxes originating from the fission reactions in the fuel. The interaction of these energetic particles with the atoms of the metallic structures displaces them from their stable positions in the crystalline lattice, thereby creating lattice defects. The nature and density of these defects is at the root of the microstructure changes suffered by materials during irradiation. These characteristics are determined by the *radiation damage* process, which is the subject of this chapter.

After the Second World War, civilian applications of nuclear power were at the forefront of technological development in society. In that context, it was recognized that radiation damage to materials used in nuclear reactors plays a large role in determining their suitability for service. E. Wigner predicted in 1946 that radiation damage would degrade material properties [1], so the term “Wigner disease” was coined to encompass the deleterious changes in material properties when exposed to irradiation by energetic particles.

Materials of interest for nuclear applications, such as metallic uranium, graphite, uranium dioxide, steels, and zirconium alloys were first developed in military programs, aimed at nuclear weapons or nuclear propulsion. Information on the properties of these materials started to be shared openly in the International Conferences for the Peaceful uses of Nuclear Energy. In parallel with these technological applications of nuclear power, physicists recognized that energetic particles could produce point defects in these solids. This inspired efforts to understand the properties of these defects by techniques such as resistivity changes and positron annihilation spectroscopy. Understanding the physical mechanisms of radiation degradation of materials is a continuing activity, not only for nuclear power industry but in many other fields, most notably the semiconductor processing industry [2, 3].

This chapter reviews the basics of radiation damage, following various previous works on the subject (see for example the proceedings of the Illinois Summer School, published in Journal of Nuclear Materials, especially the article by Mark Robinson [4]).

12.2 Particle-Solid Interactions

It is useful to divide the effect of an external flux of energetic particles in a metal into two components: (i) creation of *primary knock-on atoms* (called PKAs – these are the first atoms that absorb momentum from a collision with an energetic particle) and (ii) creation

of transmuted atoms through nuclear reactions. Both of these processes result from the interaction of the particles with the atoms in the solid, as shown in Figure 12.1.¹

¹ Note that in insulator materials it is possible to have other types of damage associated with charge deposition. For example the creation of fission tracks in materials whereby an energetic ion may leave behind a trace of its passage in the material (see Fig.15.6, [5] D. R. Olander, *Fundamental Aspects of Nuclear Reactor Fuel Elements*: ERDA, 1976.).

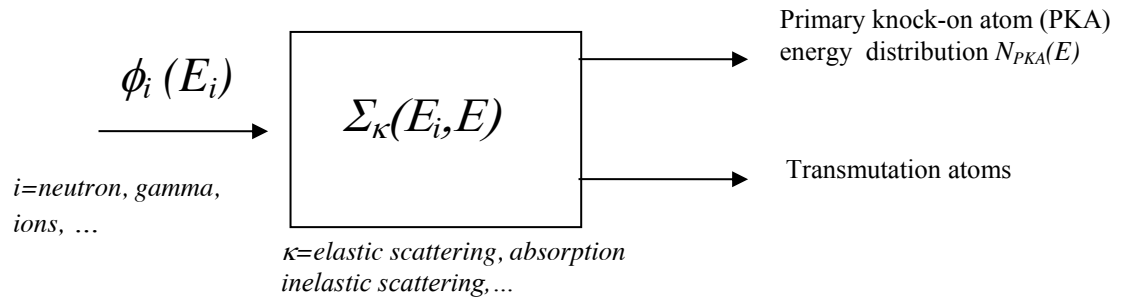


Fig. 12.1: The interaction of particles with atoms in the solid

In Fig. 12.1, $\phi_i(E_i)$ represents the flux of particle i which varies with particle energy E_i ($i=neutron, gamma, ..$), while $\Sigma_{\kappa}(E_i, E)$ is a measure of the probability of interaction (the macroscopic cross-section) of the various κ particle-solid reactions, transferring energy E to the atoms in the solid Fig. 12.1). The product of the interaction of the flux of energetic particles (represented by ϕ) and the atoms in the solid (represented by Σ) is the creation of a distribution of $N_{PKA}(E)$ self-atom recoils called primary knock-on atoms (PKAs) and a concentration of transmutation atoms C_k , where k represents the atomic species created.

Among the many processes that can cause atomic displacements in solids under the flux of energetic particles, the largest contributor to displacement damage of structural components in reactor cores is the fast-neutron flux $\phi_n(E_n)$ interacting by elastic scattering (Σ_s) with the atoms in the solid, creating a distribution of PKAs, which in turn displace other atoms.

12.2.1 Cross section

The probability of occurrence of a particular reaction between the atoms in the solid and the incident particle flux is represented by a *cross-section*. The concept of the *microscopic* cross-section is illustrated in figure 12.2. The microscopic cross section attributes an apparent *size* to the atoms in the solid proportional to the measured reaction rates, such that for a given particle flux spectrum into a solid of a given atomic density the apparent particle size increases with the probability of reaction. Figure 12.2 shows two types of atoms present in the solid: atom A has a greater reaction rate for reaction 1 than atom B, and thus the former appear very large when reaction 1 is considered. In contrast, for reaction 2, atom B has a much larger cross section and consequently these atoms appear bigger when reaction 2 is considered.

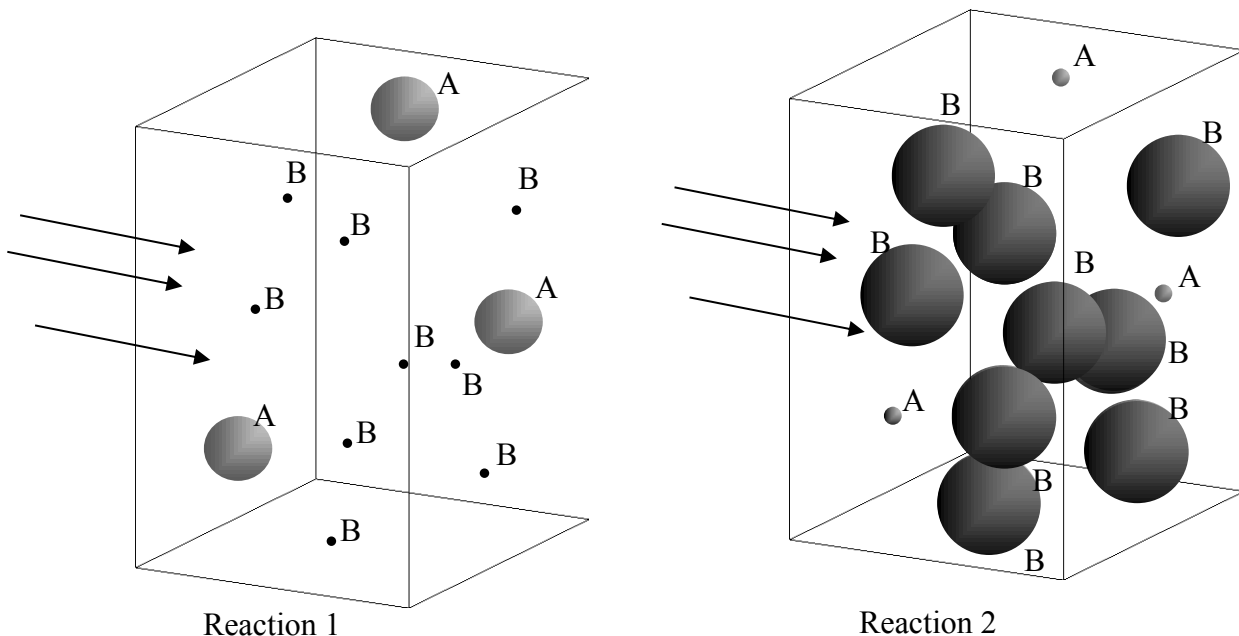


Fig. 12.2: Schematic representation of the microscopic cross-section concept. If A atoms are U-235 and B atoms are B-10, then on the left reaction 1 would be nuclear fission for which the U-235 atoms have a large cross section and the B atoms not, while reaction 2 on the right could be the (n, α) reaction for which the cross section of U-235 is much smaller than that of B-10.

If for example we let atom A (light atoms) be uranium-235 and atom B (dark atoms) be boron-10, and let Reaction 1 be nuclear fission and Reaction 2 the (n, α) reaction (absorption of neutron and emission of an alpha particle), in a thermal neutron flux the microscopic cross sections qualitatively appear as shown in Fig.12.2.

The unit of the microscopic cross-section is the barn (10^{-24} cm^2). The *macroscopic* cross-section $\Sigma \text{ (cm}^{-1}\text{)}$ is the product of the microscopic cross-section $\sigma(E_i) \text{ (cm}^2\text{/atom)}$ and the atomic density $c \text{ (cm}^{-3}\text{)}$. The usefulness of the cross section concept comes from the fact that when multiplied by a particle flux ($\text{particle.s}^{-1}.\text{cm}^{-2}$), the reaction rate $\phi\Sigma \text{ (reactions.s}^{-1}.\text{cm}^{-3}\text{)}$ is obtained.

In a solid containing c target atoms per unit volume through which passes a single particle of energy E_i , the differential probability dP that this particle will interact with one of the target atoms in an element of small thickness dx is given by:

$$dP = c\sigma(E_i)dx = \Sigma dx \quad (12.1)$$

Equation (12.1) is valid for any atomic reaction (absorption, fission, scattering, etc.). If $\sigma(E_i)$ is an elastic scattering cross section, then the result of such an interaction is transfer of energy E from the energetic particle to the struck atom, which then becomes an energetic recoil atom, called the primary knock-on atom (PKA). The PKA energy distribution $N_{\text{PKA}}(E)$ is the primary means of characterizing the damage caused by irradiation.

Fast neutrons passing through a solid can scatter elastically or inelastically, and thermal neutrons can induce nuclear reactions, all of which deposit energy onto the material. The first result of a neutron-atom interaction is the formation of a PKA followed by production of secondary recoils from the PKA, according to:

$$\begin{array}{ccccc} E_n & \Rightarrow & E & \Rightarrow & T \\ \text{Neutron} & \Rightarrow & \text{PKA} & \Rightarrow & \text{Secondary Recoils} \end{array}$$

The problem of calculating the displacement damage can be divided into the tasks of (i) finding the energy spectrum of the PKA created by interaction of the neutrons with the atoms of the solid and (ii) calculating the damage that a PKA of a given energy can produce. We address the second question in the next few sections and later in the chapter we consider the first.

12.3. Primary Knock on Atom (PKA) Energy Loss Mechanisms

To find the number of displacements caused by a PKA it is first necessary to compute the energy transferred by the energetic PKA to the neighboring atoms .

The total rate of energy loss of a PKA of energy E moving through a solid can be separated into three components:

$$\left. \frac{dE}{dx} \right|_{\text{TOTAL}} = \left. \frac{dE}{dx} \right|_E + \left. \frac{dE}{dx} \right|_N + \left. \frac{dE}{dx} \right|_I \quad (12.2)$$

where the terms on the RHS of Eq (12.2) refer to *electronic* energy loss (E), *nuclear-elastic* scattering (N) and *nuclear-inelastic* scattering (nuclear reactions) (I). Because the typical PKA energies in recoil spectra generated during reactor irradiation are considerably lower than the energies required for nuclear inelastic scattering, the first two processes dominate energy loss in most materials of interest. In metals, because the electrons are shared by all atoms in the lattice, the collisions with electrons are of little permanent consequence to the solid; the energy of high-speed electrons is degraded into heat. In insulators or materials used in the electronics industry, however, electronic damage can be significant [2]. . Nuclear-elastic scattering can cause permanent damage to the crystal in the form of atomic displacements. The partition between these two forms of energy loss determines the amount of radiation damage to metals and the subsequent radiation effects observed. We now consider these processes in turn.

12.3.1 Binary Elastic Collision Dynamics

The process of elastic transfer of energy is akin to hard sphere collisions, similar to what occur in billiard balls. We derive here the energy transfer between two hard spheres that collide. Figure 12.3 shows the energy transfer between two colliding hard spheres in the laboratory frame of reference. An atom of mass M_1 and velocity v_{10} strikes a stationary atom of mass M_2 . After the collision, the scattering angles are ϕ_1 and ϕ_2 and velocities are v_{1F} and v_{2F}

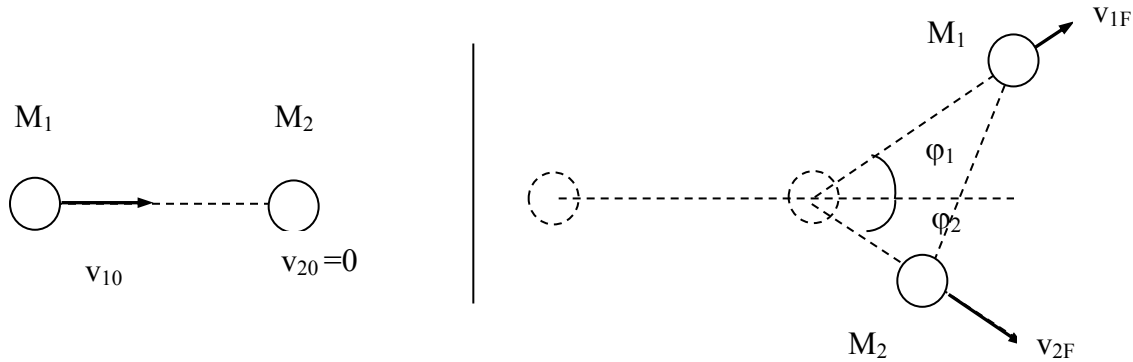


Fig. 12.3: Elastic scattering process in the laboratory frame of reference.

In the center of mass system, the above collision is shown as:

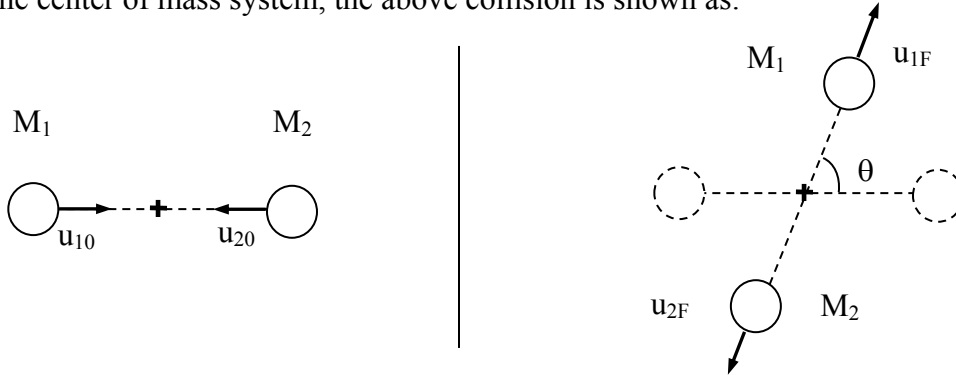


Fig. 12.4: Elastic scattering in the center of mass frame of reference.

The center of mass has the total mass of the system (M_1+M_2) so that from conservation of momentum from one frame of reference to another, the center of mass velocity v_{CM} is:

$$v_{CM} = \frac{M_1}{(M_1 + M_2)} v_{10} \quad (12.3)$$

Using conservation of kinetic energy and momentum between two instants, the first before the collision and the second after the collision, the following relations apply in the center of mass system:

$$M_1 u_{10} = M_2 u_{20} \quad (12.4)$$

$$M_1 u_{1F} = M_2 u_{2F} \quad (12.5)$$

$$\frac{1}{2} M_1 u_{10}^2 + \frac{1}{2} M_2 u_{20}^2 = \frac{1}{2} M_1 u_{1F}^2 + \frac{1}{2} M_2 u_{2F}^2 \quad (12.6)$$

where $u_{10} = v_{10} - v_{CM}$ and $u_{20} = -v_{CM}$

Substituting Eqs (12.4) and (12.5) into (12.6) we obtain $u_F = u_0$ for both particles, and thus $u_{2F} = v_{CM}$. From the definition of the center of mass velocities and noting that u_{1F} and u_{2F} have the same orientation but opposite directions, the following vectorial relationship exists for the velocities

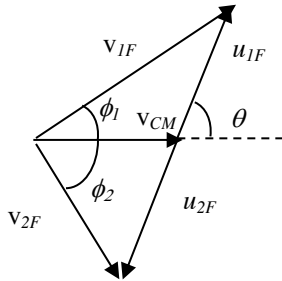


Figure 12.5 Relationship between velocities in the center of mass and laboratory frame of reference. $\vec{v}_{2F} = \vec{v}_{CM} + \vec{u}_{2F}$

Using the law of cosines:

$$v_{2F}^2 = v_{CM}^2 + u_{2F}^2 - 2v_{CM}u_{2F} \cos \theta \quad (12.7)$$

but since $v_{CM} = u_{2F}$

$$v_{2F}^2 = 2v_{CM}^2(1 - \cos \theta) \quad (12.8)$$

multiplying by $M_2/2$, and substituting for v_{CM} we obtain

$$E_{2f} = \frac{M_2}{2} v_{2F}^2 = 2 \frac{M_2}{2} \left(\frac{M_1}{M_1 + M_2} \right)^2 v_{10}^2 (1 - \cos \theta) = \frac{1}{2} \left(\frac{4M_1 M_2}{(M_1 + M_2)^2} \right) (E_{10}) (1 - \cos \theta) \quad (12.9)$$

Eq (12.9) describes the energy E_{2f} transferred to an atom of mass M_2 by an energetic particle energy E_{10} and mass M_1 as a function of the scattering angle in the center of mass system

$$\Lambda_{M_1 M_2} = \frac{4M_1 M_2}{(M_1 + M_2)^2} \quad (12.10)$$

Noting that the initial kinetic energy of particle 1 is $E_{10} = \frac{1}{2} M_1 v_{10}^2$:

$$E_{2f} = \frac{1}{2} \Lambda E_{10} (1 - \cos \theta) \quad \text{or if } E_{2f} = T \text{ and } E_{10} = E$$

$$T = \frac{1}{2} \Lambda E (1 - \cos \theta) \quad (12.11)$$

The maximum amount of energy transferred occurs for a head-on collision in which $\theta = \pi$ and

$$T_{\max} = \Lambda E \quad (12.12)$$

The energy transferred changes with the mass ratio of the energetic particle and the struck atom. For atoms of equal mass $\Lambda=1$, that is, in a head-on elastic collision the incoming atom transfers all of its energy to the struck atom. As the masses become increasingly different, the maximum possible transferred energy Λ decreases and as a consequence T_{\max} also decreases.

Example #1 Energy transfer from neutrons to Fe-C

In steel (Fe-C) under 1 MeV neutron irradiation the maximum energy transfer from the neutron to the carbon atom is $E_{n-C}=0.28 E_n$ (280 keV) and $E_{n-Fe}=0.07 E_n$ (70 keV). Thus in an elastic collision, a 1 MeV neutron can only transfer 70 keV to an iron atom. The 280 keV C primary knockon atom can transfer up to 100% of its energy to another C atom but only $T_{C-Fe}=0.58 E_{n-C}$ (162 keV) to an Fe atom. The 70 keV Fe primary knock-on atom can transfer up to 100% of its energy to another Fe recoil atom but only $T_{Fe-C}=0.58 E_{n-Fe}$ (40.6 keV) to a C atom.

12.3.2. The limit between nuclear and electronic stopping

Because the electronic density in the material is far greater than the atom density, as long as the energetic particles can transfer energy to the electrons, they preferentially do so. In order for the electrons to be able to accept the energy from the moving particle, they need to receive an energy equal to or greater than their ionization energy. For metals, since the average kinetic energy of the conduction electrons is about 3/5 of the Fermi energy ϵ_F , the ionization energy (I) is approximately equal to 2/5 ϵ_F . A simple way to estimate the

energy transferred to an electron in a collision between an particle of mass M and energy E is to use Eq (12.12):

$$T_e^{\max} = \Lambda_{M-e} E \cong \frac{4m_e}{M} E \quad (12.13)$$

Setting $T_e^{\max} = I$ (ionization energy) we obtain the minimum PKA energy for electronic-energy transfer

$$E > E^* = \frac{M}{4m_e} I \quad (12.14)$$

The value of 5 eV is a good approximation of the Fermi energy in metals and thus $I \sim 2$ eV; if we take $m_e = \frac{1}{1840} amu \cong \frac{1}{2000} amu$, then we obtain a convenient formula for the cutoff energy:

$$E^* \cong 1000 \times M_1 [eV] = \mathcal{M} [keV] \quad (12.15)$$

Thus, the cutoff energy for electronic energy loss E^* is numerically equal to the atomic mass \mathcal{M} , expressed in units of keV. For example, according to the model a $^{56}_{26}Fe$ atom traveling through a solid starts losing energy to nuclei below ~ 56 keV.

Clearly, electronic energy loss continues to occur to some extent below E_{\min} , in parallel with nuclear stopping, but it is difficult to evaluate its exact contribution. It is possible, however to estimate this energy partitioning by Monte Carlo computer simulation. The computer programs TRIM (TRansport of Ions in Matter) and SRIM (Stopping and Range of Ions in Matter), [6], are Monte Carlo programs that use specially developed interatomic potentials to calculate the energy deposition of energetic atoms in solids. Both electronic and nuclear stopping are treated simultaneously to achieve a more realistic energy partition (see section 12.9.3)

12.3.3. Electronic Stopping: energy transfer rate

The energy transfer from a PKA energy E , mass M to the electrons in the solid is now considered. The transfer is calculated differently depending on the ion energy. Although energy transferred to electrons causes no permanent damage in metals, it is important to calculate the partition between electronic and nuclear stopping as the latter does produce permanent damage.

For a high energy ions, (in which the ion velocity $v_I > 3 v_{EL}$, velocity of electrons), as the atom travels through the solid, some of its electrons are stripped off, causing the atom to become a charged particle of effective charge Z_{eff} . Because the effective charge changes with atom energy, it constantly changes as the atom loses energy while traveling through the solid. If Z_{eff} is known, then the Bethe formula gives an approximate expression for the electronic energy loss of the moving ion:

$$\left. \frac{dE}{dx} \right|_{EL} = \frac{2\pi n_e Z_{eff}^2 e^4 (M / m_e)}{E} \ln \left[\frac{4E}{(M / m_e) \bar{I}} \right] \quad (12.16)$$

where n_e is the electron density, e is the electron charge, and \bar{I} the average ionization energy in the metal. The value of the effective charge was computed by Bohr as

$$Z_{eff} = \frac{Z^{1/3} \hbar}{e^2} \left(\frac{2E}{M} \right)^{1/2} \quad (12.17)$$

where \hbar is Planck's constant divided by 2π , and Z is the atomic number of the energetic particle.

For low energy ions the energy transfer to an electron in an ion-electron collision is

$$T_e = \frac{1}{2} m_o (v_{ef}^2 - v_e^2) \quad (12.18)$$

where v_{ef} and v_e are the final and initial electron velocities, and m_o is the rest mass of the electron. But, from conservation of momentum,

$$v_1 + v_e = v_{ef} - v \text{ and } \therefore v_{ef} = v_e \left(\frac{2v}{v_e} + 1 \right) \quad (12.19)$$

where v is the PKA velocity. Thus,

$$T_{EL} \cong 2m_o v v_e = 2m_o \sqrt{\frac{2E}{M_1}} \sqrt{\frac{2 \times (3\epsilon_F / 5)}{m_o}} = A\sqrt{E} \quad (12.20)$$

The energy transfer rate (called the stopping power) is given by:

$$\left. \frac{dE}{dx} \right|_e = \frac{\text{collisions}}{PKA.s} \times \frac{\text{energy lost}}{\text{collision}} \div \frac{\text{distance travelled}}{PKA.s} = (\sigma_e J_e) \times (T_e) \div (v) \quad (12.21)$$

where σ_e is the cross section for atom-electron scattering, J_e is the flux of electrons seen by the moving PKA and is equal to $J_e = n_e (v_e + v) \cong n_e v_e$ for low energy PKAs, but

since below the Fermi level all states are occupied, the “excitable” fraction of electrons is $n_e = \frac{T_e}{\mathcal{E}_F} N_e$ where N_e is the total electron density in the material.

Since the average electron initial kinetic energy is $3/5 \mathcal{E}_F$, and

$$\left. \frac{dE}{dx} \right|_e = (\sigma_e J_e) \times (T_e) \div (v_1) = \sigma_e \left(\frac{T_e}{\mathcal{E}_F} N_e v_e \right) (2m_o v v_e) / v_1 = 2.4 \sigma_e N_e T_e \quad (12.22)$$

But $T_e = A\sqrt{E}$, and for a given material, the cross section for electron-ion collisions varies slowly with energy, and the other terms are constant, so that in the electron-stopping region the energy loss rate by the PKA is proportional to the square root of the PKA energy:

$$\left. \frac{dE}{dx} \right|_e = K\sqrt{E} \quad (12.23)$$

According to detailed calculations by Lindhard:

$$K = 0.3c_a Z^{2/3} \left[\frac{\sqrt{eV}}{A} \right] \quad (12.24)$$

where c_a is the atomic density (nm^{-3}) and Z is the atomic number. Thus, in the electron stopping region the energy loss rate by the PKA is approximately proportional to the square root of the PKA energy.

12.3.4. Nuclear stopping

When the energetic particle (PKA) slows down enough that energy transfer to the electrons becomes difficult, it starts to lose energy by collisions with the nuclei in the solid causing lattice displacements. For elastic collisions, a PKA with energy E strikes an atom in the solid, and transfers energy T , leaving it with energy $E-T$. The moving atom can transfer to the atom in the solid any energy between 0 and ΛE . The probability that a particle with energy between E and $E+dE$ transfers to an atom in the solid an energy between T and $T+dT$ is given by the differential energy-transfer cross section $\sigma(E,T)$.

The differential cross section $\sigma(E,T)$ and the total cross section $\sigma(E)$ are related by

$$\sigma(E) = \int_0^{\Lambda E} \sigma(E,T) dT \quad (12.25)$$

The average energy loss dE in dx is given by integrating Eq (12.25) over all possible values of the transferred energy T :

$$dE = \int_0^{T_m} c\sigma(E,T)TdTdx \quad (12.26)$$

the nuclear stopping power is given by

$$\left. \frac{dE}{dx} \right|_N = \int_0^{\Lambda E} c\sigma(E,T)TdT \quad (12.27)$$

The detailed process of atomic scattering and the energy loss for a single collision can be derived more exactly than in section 12.3.1. Using conservation of energy and momentum a relationship between the scattering angle in the center of mass system and the impact parameter is derived in the following section.

12.3.5 . Ion-Atom Scattering; General Binary Collision Dynamics

A collision between two particles with a interaction potential $V(r)$, and which collide with an impact parameter p is shown in Fig. 12.6. It is desired to find the orbit of two particles in an elastic collision and to relate the interaction potential to the differential cross section $\sigma(E,\theta)$.

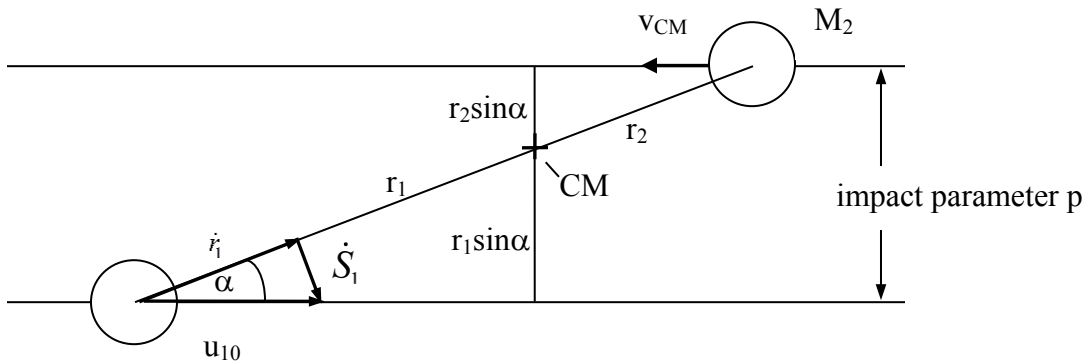


Fig. 12.6: Geometry for derivation of elastic collision between an energetic ion and a stationary atom, interacting by a potential $V(r)$.

In the system considered, a particle mass M_1 is moving initially with kinetic energy E towards an initially-stationary particle mass M_2 . The center of mass CM is located on the line joining the two masses at a distance

$$r_1 = \frac{M_2}{M_1 + M_2} r \quad \text{and} \quad r = r_1 + r_2 \quad (12.28)$$

from the mass M_I . The velocity of particle 1 in the center-of-mass system, u_{10} , is decomposed into two perpendicular components \dot{r}_1 and \dot{S}_1 , such that $\vec{u}_{10} = \vec{\dot{S}}_1 + \vec{\dot{r}}_1$. The line between the particles makes an angle α with the initial direction of the particles in the CM system. Only the initial kinetic energy in the CM system is convertible to potential energy, and this is written

$$E_{CM} = \frac{1}{2}(M_1 + M_2)v_{CM}^2 \quad (12.29)$$

and using Eq (12.3):

$$E_{CM} = \frac{M_1}{M_1 + M_2} E = \frac{M_1}{M_1 + M_2} \left[\frac{M_1 v_{10}^2}{2} \right] \quad (12.30)$$

where E is the initial kinetic energy of particle 1 in the laboratory frame. Now using conservation of energy and angular momentum during the collision it is possible to derive a relationship between the scattering angle in the center of mass θ and the impact parameter p . The trajectory of the particles as they interact and are deflected by angle θ as shown in Fig. 12.7.

Conservation of Energy

As the two energetic particles approach each other they convert kinetic energy into potential energy, $V(r)$, so that at the distance of closest approach the kinetic energy is minimized. Conservation of energy for the system is:

$$E_{CM} = V(r) + \frac{1}{2} M_1 u_{10}^2 + \frac{1}{2} M_2 u_{20}^2 = V(r) + \frac{1}{2} M_1 (\dot{r}_1^2 + \dot{S}_1^2) + \frac{1}{2} M_2 (\dot{r}_2^2 + \dot{S}_2^2) \quad (12.31)$$

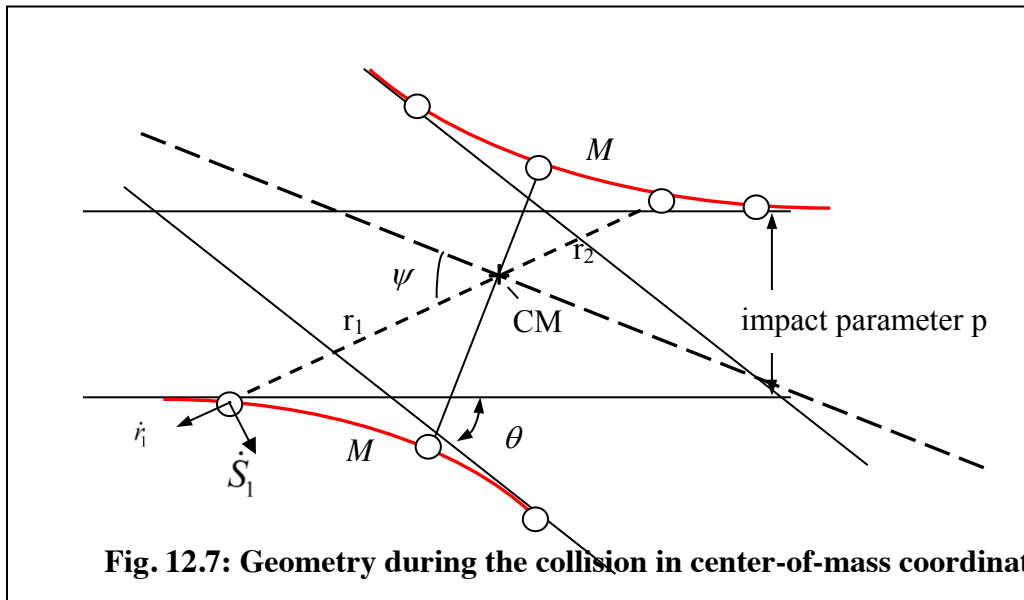


Fig. 12.7: Geometry during the collision in center-of-mass coordinates.

The tangential speed \dot{S} is equal to $r\dot{\psi}$, so Eq (12.31) is:

$$E_{CM} = V(r) + \frac{1}{2} M_1 (\dot{r}_1^2 + r_1^2 \dot{\psi}^2) + \frac{1}{2} M_2 (\dot{r}_2^2 + r_2^2 \dot{\psi}^2) \quad (12.32)$$

and using the definition of the energy of the center of mass,

$$E_{CM} = V(r) + \frac{1}{2} \left(\frac{M_1 M_2}{M_1 + M_2} \right) (\dot{r}^2 + r^2 \dot{\psi}^2) \quad (12.33)$$

along with:

$$\dot{r}^2 = \left(\frac{dr}{d\psi} \frac{d\psi}{dt} \right)^2 = \left(\frac{dr}{d\psi} \right)^2 \dot{\psi}^2 \quad (12.34)$$

yields:

$$E_{CM} = V(r) + \frac{1}{2} \left(\frac{M_1 M_2}{M_1 + M_2} \right) \left(\left[\frac{dr}{d\psi} \right]^2 + r^2 \right) \dot{\psi}^2 \quad (12.35)$$

Conservation of Angular Momentum

The angular momentum of a mass M about an axis is $\vec{r} \times (M\vec{u}) = rMu \sin \alpha = rM\dot{S}$ where r is the distance between the particle and the axis, u is the velocity and α is the angle between r and u . Then, the total angular momentum in the CM system is equal to

$$L = r_1 M_1 u_{10} \sin \alpha + r_2 M_2 v_{CM} \sin \alpha \quad (12.36)$$

The tangential velocity \dot{S} is equal to $r\dot{\psi}$ and thus

$$L = L_1 + L_2 = M_1 \dot{S}_1 r_1 + M_2 \dot{S}_2 r_2 = M_1 r_1^2 \dot{\psi} + M_2 r_2^2 \dot{\psi} \quad (12.37)$$

Using the definition of CM velocity in Eq (12.36) and equating to Eq (12.37)

$$L = \frac{M_1 M_2}{M_1 + M_2} v_{10} (r_1 \sin \alpha + r_2 \sin \alpha) = \frac{M_1 M_2}{M_1 + M_2} v_{10} p = M_1 r_1^2 \dot{\psi} + M_2 r_2^2 \dot{\psi} \quad (12.38)$$

using Eqs (12.28) in Eq (12.38) we obtain an equation for $\dot{\psi}$

$$\dot{\psi} = v_{10} p / r^2 \quad (12.39)$$

which can be eliminated in Eq (12.38)

$$E_{CM} = V(r) + \frac{1}{2} \left(\frac{M_1 M_2}{M_1 + M_2} \right) \left(\left[\frac{dr}{d\psi} \right]^2 + r^2 \right) \left(\frac{v_{10} p}{r^2} \right)^2 \quad (12.40)$$

Using Eq (12.30) to eliminate v_{10} :

$$\frac{d\psi}{dr} = \frac{p}{r^2} \frac{1}{\left[1 - \frac{V(r)}{E_{CM}} - \frac{p^2}{r^2} \right]^{1/2}} \quad (12.41)$$

When the particles are at their closest, $r=r_o$ and $\psi=\pi/2$, and when $r \rightarrow \infty$, $\psi \rightarrow \theta/2$. Integrating Eq (12.41) from the distance of closest approach to infinity:

$$\int_{\theta/2}^{\pi/2} d\psi = \frac{\pi}{2} - \frac{\theta}{2} \quad (12.42)$$

produces the *Classical Scattering Integral*

$$\theta = \pi - 2 \int_{r_o}^{\infty} \frac{p dr}{r^2 \left[1 - \frac{V(r)}{E_{CM}} - \frac{p^2}{r^2} \right]^{1/2}} \quad (12.43)$$

Equation (12.43) relates the impact parameter p to the scattering angle in the center of mass θ . At the distance of closest approach $dr/d\psi=0$ and

$$1 - \frac{V(r_o)}{E_{CM}} - \frac{p^2}{r_o^2} = 0 \quad (12.44)$$

Equation (12.44) can be solved for the distance of closest approach as a function of impact parameter. In a head-on collision $p=0$ and Eq (12.44) reduces to $V(r_o)=E_{CM}$, which, using Eq (12.27) yields the distance of closest approach in a head-on collision.

Relation of Impact parameter to Differential cross section

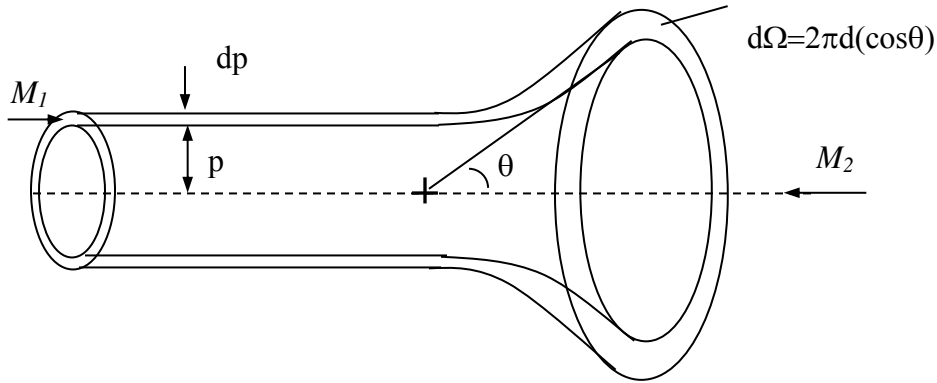


Fig. 12.8: The geometry of the differential cross section.

As shown in Fig. 12.8, if the impact parameter is in the range p to $p+dp$, the annular ring of area $2\pi p dp$ is the area associated with the annular cone $2\pi\sigma(E,\theta)d(\cos\theta)$ and thus

$$\sigma(E,\theta) = \frac{1}{2} \frac{dp^2}{d(\cos\theta)} \quad (12.45)$$

If the potential $V(r)$ is known, then Eq (12.43) can be integrated to give the final orbit of the particle after the scattering event, i.e., θ as a function of p . Then Eq (12.45) determines the cross section. This process can be performed analytically for a few simple potentials, but in most cases numerical integration is necessary. One of the analytical cases is the well-known Rutherford cross section, which is derived in Example #2.

Example # 2 Rutherford Cross Section

Substituting the unscreened Coulomb potential

$$V(r) = \frac{Z_1 Z_2 e^2}{r} \quad (12.46)$$

into Eq (12.43) gives:

$$\frac{\theta}{2} = \frac{\pi}{2} - P \int_0^1 \frac{du}{[1 - \alpha u - p^2 u^2]^{1/2}} \quad (12.47)$$

where

$$u = \frac{r_o}{r} \quad \alpha = \frac{C}{r_o E_{CM}} \quad C = Z_1 Z_2 e^2 \quad P = \frac{p}{r_o} \quad (12.48)$$

The solution of Eq (12.47) is

$$\frac{\theta}{2} = \frac{\pi}{2} - \sin^{-1} \left(\frac{\alpha + 2P^2}{\sqrt{\alpha^2 + 4P^2}} \right) + \sin^{-1} \left(\frac{\alpha}{\sqrt{\alpha^2 + 4P^2}} \right) \quad (12.49)$$

The dimensionless form of Eq (12.44) is

$$P^2 = 1 - \alpha \quad (12.50)$$

Using Eq (12.50), Eq (12.49) reduces to

$$\alpha = \frac{2 \sin(\theta/2)}{1 + \sin(\theta/2)} \quad (12.51)$$

Substituting Eqs (12.48) and (12.51) into (12.50) yields:

$$p^2 = \frac{C^2}{4E_{co}^2} \left(\frac{1 + \cos \theta}{1 - \cos \theta} \right) \quad (12.52)$$

The impact parameter $p \rightarrow 0$ as $\theta \rightarrow \pi$ (head-on collision) and as $\theta \rightarrow 0$ $p \rightarrow \infty$ (complete miss).

Substituting Eq (12.52) into Eq (12.45), results in the *Rutherford cross section*:

$$\sigma(E, \theta) = \frac{Z_1^2 Z_2^2 e^4}{16E^2} \left(\frac{M_1 + M_2}{M_2} \right)^2 \frac{1}{\sin^4(\theta/2)} \quad (12.53)$$

which can be converted into a energy transfer cross section by noting that

$$\sigma(E, T) = \left[\frac{2\pi d(\cos \theta)}{dT} \right] \sigma(E, \theta) = \frac{4\pi}{\Lambda} \sigma(E, \theta) \quad (12.54)$$

Combining Eqs (12.53) and (12.54) yields:

$$\sigma(E, T) = \pi Z_1^2 Z_2^2 e^4 \left(\frac{M_1}{M_2} \right) \frac{1}{ET^2} \quad (12.55)$$

The Rutherford cross-section decreases with increasing PKA energy. Note also that small scattering angles (which correspond to small values of the transferred energy T) are strongly favored. The Rutherford cross-section is based on an unrealistic unscreened potential, which cause the energetic particle to interact with the nuclei in the material as if the electrons did not exist. In reality particle-atom Coulomb interactions are screened by the electrons, the degree of screening decreasing with increasing particle energy.

So far we have examined the stopping process from the point of view of the energetic particle as it deposits energy in the solid. While the electronic energy loss does not lead to permanent accumulation of damage, the nuclear energy loss can in fact displace atoms

from their equilibrium lattice positions. This process by which the deposited energy results in displacements is described in the next section.

12.4. The Displacement Process

12.4.1. Threshold Displacement Energy

As a result of scattering by energetic particles, atoms in the solid are displaced from their equilibrium lattice positions, creating a vacant lattice site and a self-interstitial atom (SIA). This vacancy-interstitial pair is called a Frenkel pair (FP).

Normally in metals the struck atom is not the one that eventually ends as a SIA; instead, the struck atom starts a *replacement collision sequence* (RCS) along one of the close packed crystallographic directions (Fig. 12.9). If the initial energy of the struck atom is too low, the collision sequence propagates along the close-packed direction but then returns each atom to its original location; if the energy is high enough, the RCS returns only partway to the original struck atom location. At the end of the chain of displaced atoms, a SIA is formed and a vacant lattice site remains at the site of the original collision of the PKA. In between, each atom displaces its neighbor in a “domino” effect. The end result is creation of a Frenkel pair.

In the recovered part of the collision sequence (right side of Fig. 12.9), only energy is transferred along the line of close-packed atoms but no atom is permanently displaced; this is called a *focusson*. The minimum energy required to sufficiently move the atoms so that they do not return to their initial sites is termed the *displacement energy* E_d . The magnitude of E_d depends on the crystallographic direction of the displacement chain. The minimum chain length to create a permanent FP is that which avoids athermal recombination (i.e. an atomic jump which occurs without requiring thermal energy). The cross-shaped enclosure in Fig. 12.9 shows schematically this recombination volume. A vacancy created inside this volume spontaneously recombines with the interstitial shown at its center.

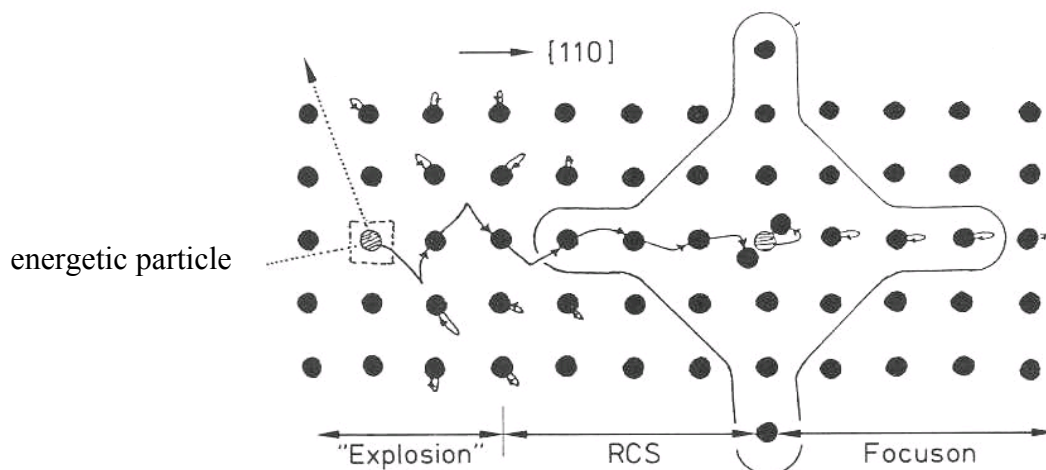


Fig. 12.9 Schematic representation of the atomic displacements involved in the creation of a permanent Frenkel pair [3]

Fig.12.9 illustrates that the displacement energy depends on the crystalline orientation. This has been demonstrated, both experimentally and computationally. Figure 12.10 shows the variation of E_d with crystalline orientation in pure Cu. The displacement energy is lowest along the low-index crystallographic directions such as $[110]$ and $[100]$ (about 20 eV in this case) but highest along $[111]$ (~ 80 eV).

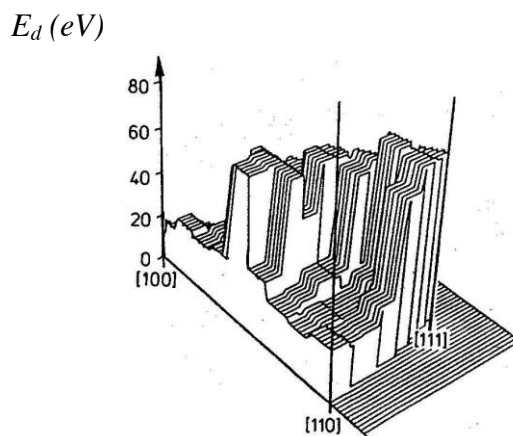


Fig. 12.10. Measured displacement energies for various RCS directions in Cu [7]

Because of the intrinsic uncertainties of displacement measurements and calculations, it is customary to use an *average* displacement energy. For metals the average displacement energy is on the order of 20-40 eV. Compilations of displacement energies for various materials can be found in [8], but it has been proposed that 40 eV be used whenever more precise knowledge does not exist [9].

For intermetallic compounds and ceramics, in which sublattices and chemical ordering exist, the displacement energies can be much higher and can vary widely depending on the atomic species or sublattice considered [10] [7]. For example the average displacement energies for the two atom types in UO_2 are quite different, $E_d \sim 25$ eV for O^{2-} and $E_d \sim 40$ eV for U^{4+} .

In addition, point defects of one type can be unstable, decaying to the other type of defect (Chap. 24). This is also true in solid solutions where displacements of the matrix and solute atoms occur at comparable rates, but if their formation energies differ widely, one type of interstitial converts to the other type, which causes the interstitial population to be enriched in one or the other type of atom.

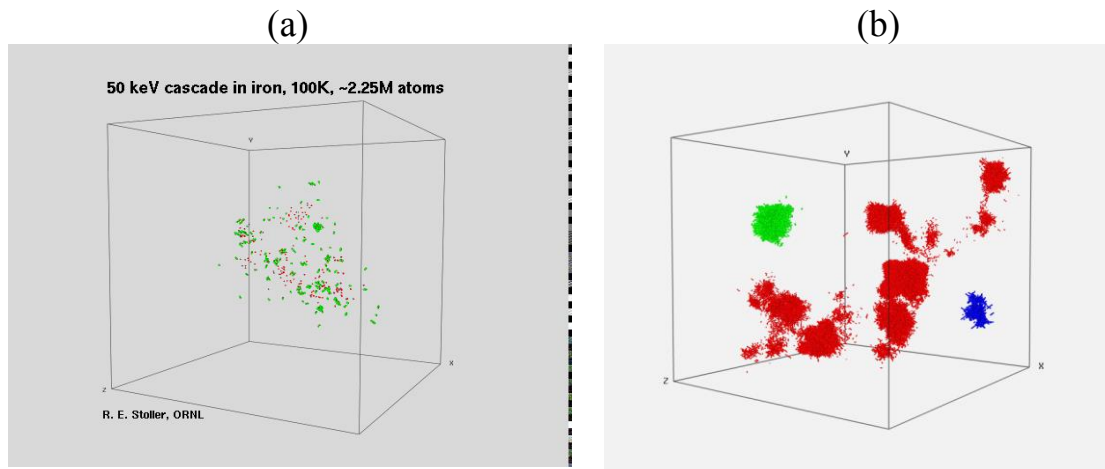


Fig. 12.11: Defect configuration after (a) a 50 keV displacement cascade in Fe, interstitials in green, vacancies in red (b) cascade substructures for PKA of different energies in Fe (5 keV blue, 10 KeV green, 100 keV red) (courtesy R. Stoller, Oak Ridge National Laboratory).

12.4.2. Displacement Cascade and the Final Damage structure

The simple picture of isolated atomic displacements described above does not hold at much higher PKA energies. As the PKA energy is divided between many atoms, a displacement cascade is formed. This is a region where the dissipation of PKA energy causes many atoms to be displaced from their lattice positions. In fact in such a case, so many atoms in a small region participate in the dissipation of energy that the very notion of crystalline lattice becomes difficult to define. In the displacement cascade region a “thermal spike” can be defined as the region in which for a brief few picoseconds the average kinetic energy of the atoms corresponds to a temperature above the melting temperature.

Figure 12.11 shows the results of a computer simulation at the end of a displacement cascade. Extensive clustering of similar point defects occurs in the cascade core, as well as recombination of interstitials and vacancies, thereby reducing the total damage.

The actual defect distribution left in the debris of the cascade should be considered. In the damage calculations later in this Chapter we divide the PKA energy equally among all atoms in the cascade, counting as permanent atomic displacements all energy transfers above E_d . In reality, because of the close proximity in which these defects are created, they interact with each other, creating defect clusters and/or restoring the undamaged lattice. This causes the final number of interstitials and vacancies to be smaller than the

total number of atoms displaced in the cascade. Since the subsequent microstructural evolution under irradiation depends on the actual number of defects and defect clusters created, it is useful to consider the physical processes occurring in the cascade.

Table 12.1 Chronology of events during the slowing down of an energetic PKA and its associated displacement cascade. (adapted from [3])

Duration (ps)	Event	Result	Parameters
10^{-3}	Transfer of energy from energetic particle	Primary knock on atom (PKA)	$\sigma(E_n, E)$ =cross section for particle energy E_n to transfer of energy E
10^{-3} to 0.2	Slowing down of PKA, generation of a displacement cascade and thermal spike	Recoil atoms and Lattice Vacancies Formation of subcascades	E_d =displacement energy v_{NRT} =number of displaced atoms T =energy transferred to recoils dpa = displacements per atom rpa =displacements per atom
0.2-3.0	Thermal spike cooldown	Stable Interstitials (SIA) Interstitial clusters Atomic mixing Athermal defect recombination	$v(T)$ =number of stable point defects f_j =clustering fraction for cluster size j rpa =replacements per atom $arc-dpa$ = athermal recombination corrected dpa
3-10	Cascade cooling to bulk solid temperature	Depleted zone in cascade core	Vacancy loop collapse probability
> 10	Thermal migration of defects and interaction with sinks	Microstructure evolution (segregation, precipitation, second phase dissolution, dislocation loop formation, etc..) leading to radiation effects (swelling, creep, embrittlement, hardening, growth, etc.)	T_{irr} =irradiation temperature E_i^m = migration energy for point defect i, i=SIA and vacancy. K_{ji} = strength of sink j for defect i FMD =Fraction of defects free for long-range migration.

The typical energy given to a PKA (on the order of keVs to 10s of keVs) is far in excess of thermal energies ($\sim 10^{-2}$ eV). Because the PKA interacts with the surrounding atoms via a screened Coulomb potential, this energy is quickly shared with other atoms, which in turn displace other atoms, until the energy per atom is smaller than the displacement energy. This process, whereby atoms in close proximity to the PKA receive large amounts of energy during a short time, originates the *displacement cascade*.

As shown in table 12.1, the initial energetic particle-target atom energy transfer occurs in about 10^{-15} s (10^{-3} ps). During the several following picoseconds, the PKA shares its energy with other nearby atoms through successive collisions. Once a few tens of atoms

participate in the cascade, a “temperature” calculated based on their average kinetic energy is far in excess of the melting temperature. Molecular-dynamics simulations (Chap. 14) show that during the first few picoseconds, the atomic configuration in the thermal spike associated with the displacement cascade is similar to that of a molten drop [8].

However, the thermal spike lasts only a few picoseconds, since the solid surrounding the cascade represents a very large reservoir which quickly dissipates the thermal energy, in effect quenching the cascade. Because of the very large difference between the PKA energies and thermal energies, the region in the material affected by the displacement cascade explores non-equilibrium crystal structures and defect configurations which are otherwise inaccessible. This causes non-equilibrium structures to appear under irradiation that are not present in purely thermal conditions.

During the “ballistic” or displacive part of cascade development, $\nu(T)$ lattice atoms are displaced from their sites. ν corresponds approximately to the value calculated from the Norgett-Robinson-Torrens model (Sect. 12.5). As illustrated in Fig. 12.12, three possible fates await the defects created by irradiation: annihilation (either by recombination or absorption at a defects sink), clustering (whereby they combine with like defects to form higher order clusters) or remaining as individual point defects.

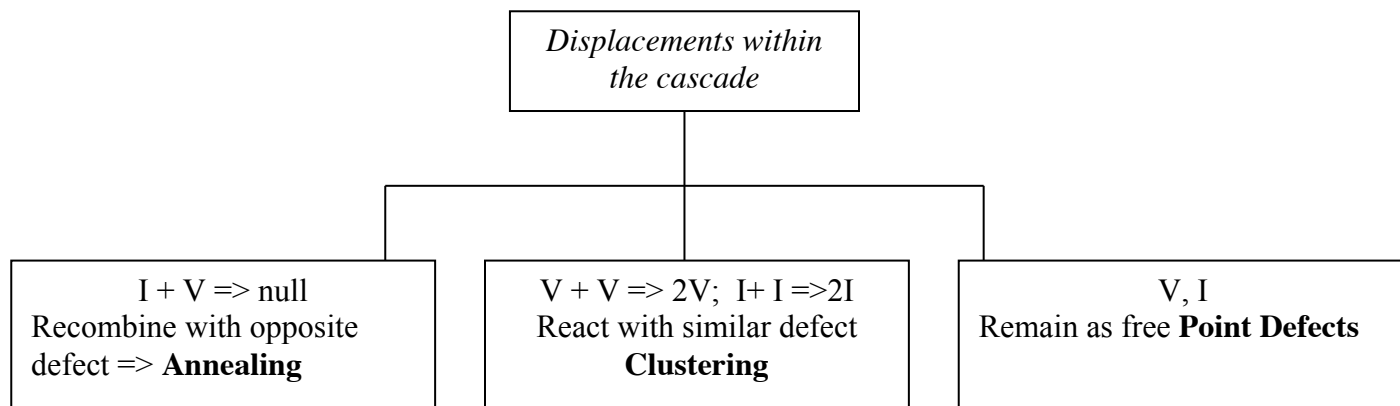


Fig. 12.12 Processes following defect creation in a displacement cascade.

As discussed in Chapter 13, the defect structure created and defect mobility at the irradiation temperature of interest determine the microstructural changes occurring under irradiation. In order to quantitatively evaluate radiation damage to solids, the number of displacements per PKA as function of its energy E is calculated in the next section.

12.5 Displacements per PKA

The final damage state results from the PKA interaction with its neighbors causing many collisions and atomic displacements followed by intra-cascade clustering and recombination. The spatial distributions of the interstitial and vacancy clusters defects are not homogeneous. Because the newly-created interstitials are energetic atoms, they are expelled from the center of the cascade via replacement collision sequences (Fig.

12.9), and a vacancy-rich core forms, along with an interstitial-rich outer shell. This physical separation between interstitials and vacancies enhances defect clustering and minimizes recombination. When the cascade cools, the final damage state contains a substantial number of point defects and point defect clusters. After this stage, the long-term interactions of the radiation damage with the remainder of the solid determine the evolution of the microstructure (Chap. 13).

The Kinchin Pease (KP) Model

The total number of displacements for a PKA energy E can be estimated by the following derivation attributed to Kinchin and Pease [11], and illustrated in Fig. 12.13. If the initial PKA energy $E > 2E_d$, the PKA causes further atomic displacements in the solid. After the first collision, the number of displaced atoms is 2 and their average energy \bar{T} is $E/2$. After the second collision, four atoms are now involved and $\bar{T} = E/4$. In general, after n collisions, 2^n atoms are involved and $\bar{T} = E/2^n$. The condition for the displacement cascade to end is that $\bar{T} \leq 2E_d$; if the energy is more than E_d and less than $2E_d$, the PKA can transfer enough energy to displace an atom, but the displaced atom is replaced by the PKA so no new defects are produced. Thus the condition

$$2E_d = \frac{E}{2^{n_f}} \quad (12.56)$$

where n_f is the final number of collisions, determines the end of the cascade. But since after n_f steps, $v=2^{n_f}$. Then the number of displacements according to Kinchin Pease is

$$v_{KP}(E) = \frac{E}{2E_d} \quad (12.57)$$




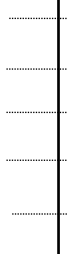
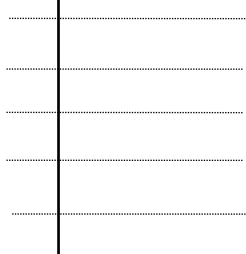


Step	0	1	2	3		n_f	FINAL
							
Average Energy per atom	E	$E/2$	$E/4$...		$E / 2^{n_f}$	$2E_d$
# of additional atoms	1	2	4	8	2^{n_f}	$E/2E_d$

Figure 12.13: Derivation of the Kinchin-Pease formula.

This is the Kinchin-Pease formula [6]. The arguments leading to Eq (12.14) and adopted in the K-P model include a sharp cutoff at an energy E^* , such that above E^* all energy loss is electronic and below E^* all energy loss is by elastic collisions with atoms. The displacements caused by such a PKA energy E are thus given by:

$$\nu(E) = \frac{E^*}{2E_d} \quad \text{if } E > E^*$$

$$\nu(E) = \frac{E}{2E_d} \quad \text{if } 2E_d < E < E^*$$

$$\nu(E) = 1 \quad \text{if } E_d < E < 2E_d$$

$$\nu(E) = 0 \quad \text{if } E < E_d$$

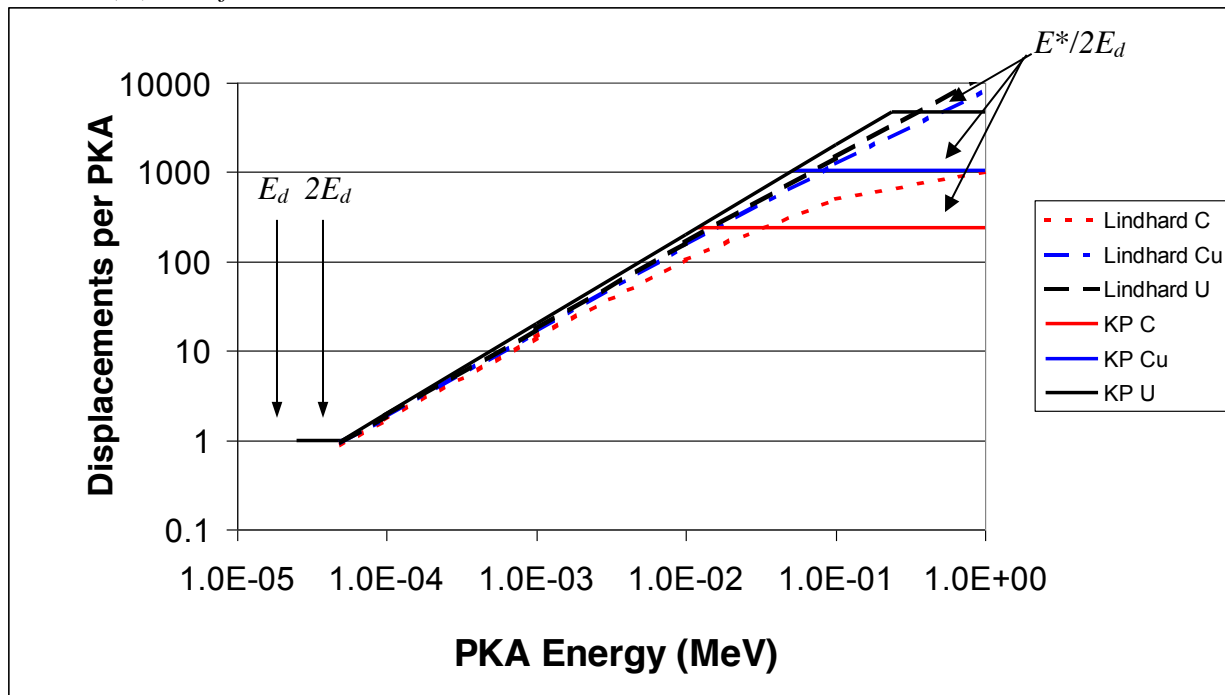


Fig. 12.14. Displacements in the Kinchin-Pease and the Lindhard models in carbon, copper and uranium.

Lindhard Scharff Schiott (LSS) Energy Partition Model

In contrast with the sharp partition used by the KP model the LSS model uses a more realistic potential (Thomas-Fermi) than the hard-sphere approximation to predict the partition between electronic and nuclear stopping. This model provides a smooth transition from the electronic-loss-dominated regime to the nuclear-stopping regime. Assuming that the nuclear stopping part of the deposited energy is converted into displacements, the number of displacements given by the LSS model, ν_{LSS} , is

$$\nu_{LSS}(E) = \zeta(E, Z) \frac{E}{2E_d} \quad (12.58)$$

$$\zeta(E, Z) = \text{damage efficiency} = \frac{1}{1 + 0.88Z^{\frac{1}{6}}(3.4\varepsilon^{\frac{1}{6}} + 0.4\varepsilon^{\frac{3}{4}} + \varepsilon)} \quad (12.59)$$

where Z is the atomic number, $\varepsilon = \frac{E}{2Z^2e^2/a}$; a = screening radius = $\frac{\sqrt{2}a_B}{(Z_1^{2/3} + Z_2^{2/3})^{1/2}}$ with a_B the Bohr radius. In the case the PKA is the same as the struck atom, the screening radius is $a = a_B/Z^{1/3}$. The damage efficiency $\zeta(E, Z)$ originates from a numerical solution of the energy partition between electronic and nuclear stopping. This solution is plotted in Fig. 12.15 and approximated by Eq (12.57)

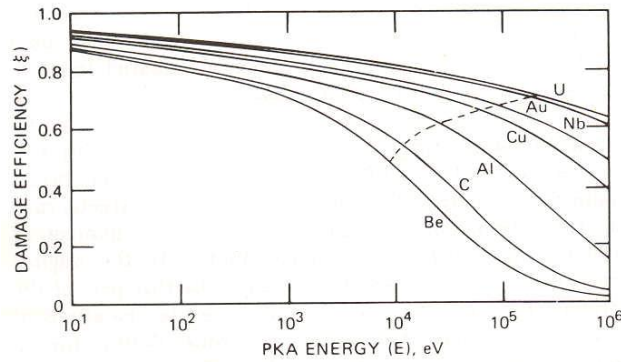


Figure 12.15: Damage efficiency as a function of PKA energy for various elements. The dashed line shows the nuclear stopping limit [10].

As seen in Fig.12.15, the damage efficiency decreases slowly with PKA energy, and decreases more steeply for light elements than heavy elements. According to Eq (12.14), the electronic stopping cutoff (dotted dashed line in figure) occurs at different energy levels for different elements. For U the damage efficiency is higher than 0.7 at the cutoff, while for Be, it is lower than 0.5.

The Norgett-Robinson-Torrens (NRT) Model

The above derivations do not take into account the fact that real collisions are not hard sphere collisions, as assumed in the Kinchin Pease model, and as specified by Lindhard, instead of the displacement process exhibiting a sharp cutoff at E^* , the partition of nuclear and electronic stopping varies smoothly with energy. Consideration of these two factors was given in deriving the Norgett-Robinson-Torrens formula [12] for the number of displacements caused by a PKA energy E , ν_{NRT} .

The nuclear and electronic partition is evaluated by using the concept of damage energy E_{dam} , which is the fraction of the recoil energy that can cause displacement damage. This is given by

The departure from hard sphere collision is evaluated by setting

$$T_{dam} = \frac{E}{(1 + k_L g(\varepsilon))} \quad (12.60)$$

where

$$k_L = \frac{32}{3\pi} \left(\frac{m_e}{M_2} \right)^{1/2} \frac{(1 + (M_2 / M_1))^{3/2} Z_1^{2/3} Z_2^{1/2}}{(Z_1^{2/3} + Z_2^{2/3})^{3/4}} \quad (12.61)$$

where M_I and Z_I indicate the mass and atomic number of the incident atom while 2 stands for the target atom. If the target and projectile are the same atom then

$$k_L = \frac{32}{3\pi} \left(\frac{m_e}{M_2} \right)^{1/2} \frac{(1 + (M_2 / M_1))^{3/2} Z_1^{2/3} Z_2^{1/2}}{(Z_1^{2/3} + Z_2^{2/3})^{3/4}} \quad (12.62)$$

$$k_L = 0.1337 Z^{1/6} \left(\frac{Z}{M} \right)^{1/2} \quad (12.63)$$

and where

$$g(\varepsilon) = \varepsilon + 0.40244 \varepsilon^{3/4} + 3.4008 \varepsilon^{1/6} \quad (12.64)$$

with

$$\varepsilon = \frac{E}{Z_1 Z_2 e^2} a_{12} \frac{(M_1 + M_2)}{M_2} = \frac{2E}{Z^2 e^2} a_{12} \quad (12.65)$$

if the atoms are the same and where e is the electron charge and the screening length a_{12} given by

$$a_{12} = \left(\frac{9\pi^2}{128} \right)^{1/3} \frac{a_B}{2^{1/2} Z^{1/3}} \quad (12.66)$$

where a_B is the Bohr radius. Using Eq. (12.60) for calculating T_{dam} , the displacements caused by the PKA energy E are

$$\nu_{NRT}(E) \cong 0.8 \frac{T_{dam}}{2E_d} \quad (12.67)$$

This formulation is used in codes that can calculate the displacements per atom for a given neutron spectrum.

The KP and NRT formulas have various limitations, for example in taking no account of collisions between atoms of different masses (for calculations of displacements in polyatomic solids see [13]) or of the variation of displacement energy with crystalline orientation. Appropriate accounting needs to be taken of electronic excitations and there

are approximations in the method above. However the greatest value of the NRT model and of other standard damage parameters (see section 12.7) is not that it gives exact numbers of displacements but, rather, that it provides a unified and consistent damage parameter that can be used to compare different types of irradiations.

In the following section the models above are used to calculate the damage produced by neutron irradiation.

12.6. Displacements per atom caused by Neutron Irradiation

In this section the atomic displacement rate caused by a given neutron flux incident on the materials of interest is calculated. The displacement rate is in units of *displacements per atom (dpa)* per second, which is simply the volumetric displacement rate (displacements per second per unit volume) divided by the atom density. In the reactor, neutrons and gamma rays bombard the nuclear fuel and reactor components. To evaluate the displacement rate k (dpa/s) in a neutron flux spectrum $\phi(E_n)$, the *displacement cross section* $\sigma_d(E_n)$ is needed. The displacement cross section is

$$\sigma_d(E_n) = \int_{E_d}^{\Lambda E_n} \sigma_s(E_n, E) \nu(E) dE \quad (12.68)$$

Once this is known the displacement rate k is given by

$$k = \int_{\frac{E_d}{\Lambda}}^{\infty} \sigma_d(E_n) \phi(E_n) dE_n \quad (12.69)$$

The lower limit of the integral represents the lowest neutron energy capable of transferring E_d to the atoms in the solid. Assuming $E_d \ll E$

$$k = \int_{\frac{E_d}{\Lambda}}^{\infty} \phi(E_n) \left[\int_0^{\Lambda E_n} \sigma_s(E_n, E) \nu(E) dE \right] dE_n \quad (12.70)$$

For isotropic scattering (all PKA energies E equally probable), and if $E_d \ll E_n$

$$\sigma_s(E_n, E) = \frac{\sigma_s(E_n)}{\Lambda E_n} \quad (12.71)$$

Substituting Eq. (12.71) into Eq. (12.68)

$$\sigma_d(E_n) = \frac{\sigma_s(E_n)}{\Lambda E_n} \int_0^{\Lambda E_n} \nu(E) dE \quad (12.72)$$

Equation (12.72) implies no dependence of σ_d on E . Substituting Eq (12.72) into Eq (12.67) gives:

$$k = \int_{\frac{E_d}{\Lambda}}^{\infty} \phi(E_n) \frac{\sigma_s(E_n)}{\Lambda E_n} \left[\int_0^{\Lambda E_n} \nu(E) dE \right] dE_n \quad (12.73)$$

To find the displacement rate caused by an incident neutron flux, it is necessary to integrate Eq (12.73) over all possible neutron energies. Any flux profile $\phi(E_n)$ or scattering cross section expression can be inserted into Eq. (12.73) to obtain realistic numbers for the displacement rate.

Using the KP expression, Eq (12.57) for $\nu(E)$, and assuming² that $\Lambda E_n < E^*$ we obtain

$$k_{KP} = \frac{\Lambda}{4E_d} \int_{\frac{E_d}{\Lambda}}^{\infty} \phi(E_n) \sigma_s(E_n) E_n dE_n \quad (12.74)$$

A simple approximation of a monoenergetic neutron flux can be used to obtain an order of magnitude of the number of atomic displacements created. The approximation consists of substituting the *total* neutron flux ϕ_t at the average neutron energy for the overall flux:

$$\phi(E_n) \cong \delta(E_n - \bar{E}_n) \phi_t \quad (12.75)$$

where $\delta(E_n - \bar{E}_n)$ is the Kronecker delta, ϕ_t is the total damage-producing neutron flux given by

$$\phi_t = \int_{\frac{E_d}{\Lambda}}^{\infty} \phi(E_n) dE_n \quad (12.76)$$

and \bar{E}_n is the average neutron energy given by

$$\bar{E}_n = \frac{\int_{\frac{E_d}{\Lambda}}^{\infty} \phi(E_n) E_n dE_n}{\phi_t} \quad (12.77)$$

and so, for a monoenergetic neutron flux of energy \bar{E}_n ,

$$k_{KP} \cong \phi_t \frac{\sigma_s(\bar{E}_n)}{4E_d} \Lambda \bar{E}_n \quad (12.78)$$

² This is a reasonable assumption since the vast majority of PKAs falls under this category. For example, the maximum energy for a PKA in Fe from a collision with a 1MeV neutron is 44 keV (< 56 keV).

Example #3 Displacements in steel

The number of displacements during one reactor cycle in a steel component subjected to a total flux of $5 \times 10^{13} \text{ n/cm}^2 \cdot \text{s}$ of monochromatic 1 MeV neutrons. For iron-neutron collisions the energy transfer parameter is:

$$\Lambda_{nFe} = \frac{4(1.56)}{(1 + 56)^2} = 0.0689$$

Using Eq (12.68) and assuming $\sigma_s = 3$ barns and $E_d = 25$ eV, we obtain

$$k_{KP} \cong 5 \times 10^{13} [\text{n} \cdot \text{cm}^{-2} \cdot \text{s}^{-1}] \frac{3 \times 10^{-24} [\text{cm}^2]}{4 \times 25 [\text{eV}]} 0.069 \times 10^6 [\text{eV}] = 1.04 \times 10^{-7} \text{ dpa/s}$$

If the reactor cycle lasts for 1.5 years ($4.73 \times 10^7 \text{ s}$) the total number of displacements per atom is $1.03 \times 10^{-7} \times 4.73 \times 10^7 = 4.87 \text{ dpa}$. Thus, according to the calculation above, during one reactor cycle, *each iron atom* in the solid is displaced on the average nearly *5 times*. Why does the solid not turn into powder after such enormous damage?

To obtain a more precise value of the displacement damage it is necessary to integrate Eq (12.64) using more realistic expressions for the scattering cross section and neutron flux. We give one such example in the example 12.3 below

Example # 4 Displacement rate in a fusion reactor first wall.

The D-T reaction in a fusion plasma produces monoenergetic 14 MeV neutrons. When these scatter from the atoms of the structure, a tail of low energy neutrons is produced, of the form

$$\varphi(E_n) = \varphi_{\max} \exp\left[\frac{-(14 - E_n)}{3}\right]$$

The above neutron flux is plotted in Fig. 12.16. For a first-wall made of Zr, the scattering cross section is given in Fig.12.17. The question posed is then what is the displacement rate at the first wall under this neutron flux?

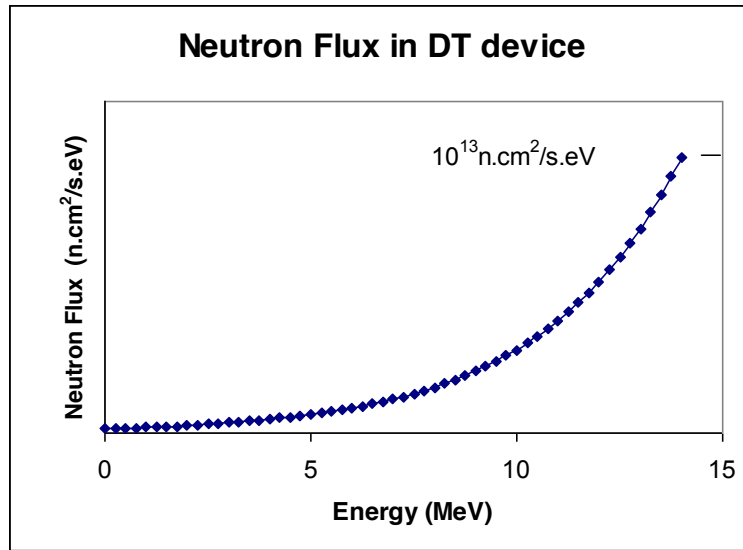


Figure 12.16: Neutron Flux for a plasma first wall in a DT fusion device

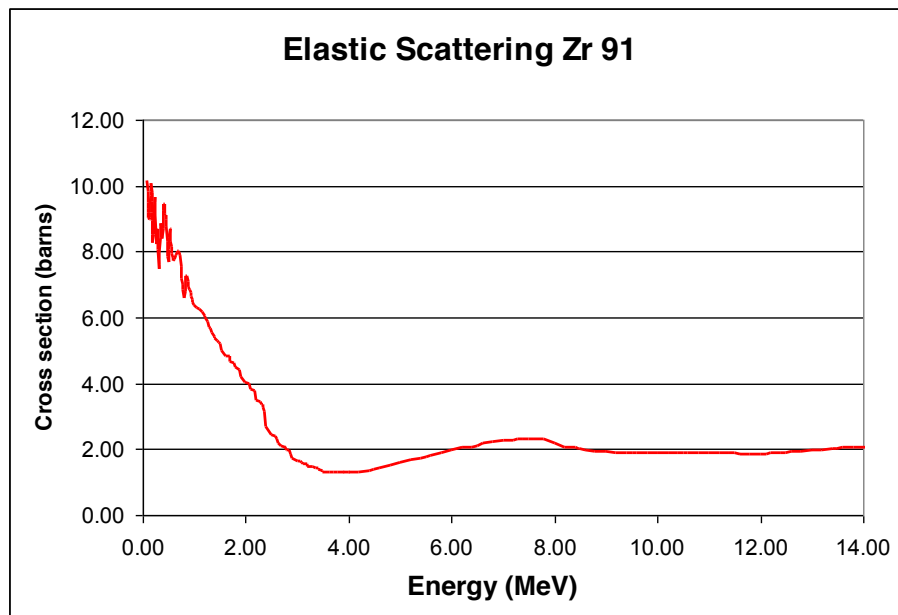


Fig. 12.17: Elastic scattering cross-section for Zr-91 [14]

For the materials of interest, $\Lambda_{\text{nZr}}=0.043$ and thus $E_d/\Lambda=581 \text{ eV}=5.81 \times 10^{-4} \text{ MeV}$. Substituting the above flux into Eq (12.64,) taking the upper integration limit as 14 MeV and considering that the scattering cross section is approximately constant (neglecting the portion below 2 MeV) and equal to $\bar{\sigma} = 2 \text{ barns}$ we obtain:

$$k_{KP} = \frac{\Lambda_{nZr}}{4E_d} \int_{\frac{E_d}{\Lambda}}^{14} \phi_{\max} \exp[-(14 - E_n)/3] E_n \sigma_s(E_n) dE_n = \frac{\Lambda_{nZr} \phi_{\max} \bar{\sigma} \exp[-14/3]}{5E_d} \int_{\frac{E_d}{\Lambda}}^{14} \exp[E_n/3] E_n dE_n$$

$$k_{KP} = \frac{\Lambda_{nZr} \phi_{\max} \bar{\sigma} \exp[-14/3]}{5E_d} \left[3(E_n - 3) \exp(E_n/3) \right]_{5.81 \times 10^{-4}}^{14} = \frac{\Lambda_{nZr} \phi_{\max} \bar{\sigma} \exp[-14/3]}{5E_d} [33 \exp(14/3) + 9]$$

which yields:

$$k_{KP} = 2.84 \times 10^{-7} \text{ dpa / s}$$

Displacements calculated with the NRT model

In estimating the neutron flux in nuclear power plants, most reactor physics calculations involve discretization of the neutron flux spectrum into individual energy groups, rather than analytical expressions. In such a calculation the displacement rate is given by the sum of the contributions of each energy group j .

Using the derivation for the displacements per recoil given by Eq. (12.67) it is possible to create a method for calculating the overall displacement rate. The first step is to divide the neutron spectrum into N energy groups, and for each neutron energy calculate a recoil spectrum will be itself divided into M energy groups. For each recoil energy the number of displacements is given by Eq. (12.67). The total number of displacements is then

$$k_{NRT} = \sum_{j=1}^N \bar{\phi}(E_n^j) \Delta E_j \sum_{k=1}^M \sigma_s^{kj}(E_n^j, E_k) \nu_{NRT}(E_k) \Delta E_k \quad (12.79)$$

with ν_{NRT} given by equation (12.67). The differential flux (or flux spectrum) $\bar{\phi}(E_n)$ has units of $(\text{n} \cdot \text{cm}^{-2} \cdot \text{s}^{-1} \cdot \text{eV}^{-1})$ and ΔE_j is the energy interval of neutron group j , while ΔE_k is the energy interval of recoil energy group k . In addition to the flux spectrum, Eq (12.79) requires recoil energy and neutron energy dependent scattering cross sections $\sigma_s^{kj}(E_n^j, E_k)$, evaluated for the equivalent energy group structure from databases such as ENDF-VI. The program SPECTER [15] takes a neutron flux such as given in Problem 12.10, and directly generates a displacement cross section compatible with the energy groups in which the flux is supplied.

12.7. Other Measures of Radiation Damage

The preceding sections have demonstrated that the number of displacements per atom is a useful measure of the damage caused by energetic particle irradiation. However, dpa is a measure only of the *total* number of displaced atoms produced in the cascade. As stated previously, as the cascade cools down a significant number of interstitials and vacancies

recombine “athermally”, that is without requiring diffusional jumps. As a result, the number of surviving defects upon cascade cooldown is much smaller than the dpa value calculated using either KP or NRT.

A recent review [16] provides estimates of the fraction of defects surviving immediate athermal recombination in the cascade (arc). This quantity is called arc-dpa and is defined as:

$$arcdpa = \xi(E)dpa \quad (12.80)$$

where

$$\xi_{arcdpa}(E) = aE^b + c \quad (12.81)$$

In equation (12.81), c is a saturation value, equal to 0.2-0.4, and b has been determined to be close to 0.8 by various groups. By setting $\xi(E) = 1$ at the beginning of the linear region, the authors find that

$$a = \frac{1-c}{(2E_d / 0.8)^b} \quad (12.82)$$

and assuming $c=0.4$ and $b=0.8$

$$\xi_{arcdpa}(E) = \frac{1-c}{(2E_d / 0.8)^b} E + c \approx \frac{0.6}{(2E_d / 0.8)^{0.8}} E + 0.4 \quad (12.83)$$

The *arcdpa* value is similar to the freely-migrating defect fraction, in that it attempts to evaluate the number of surviving defects after cascade cooldown. These are the defects that are available for long range migration and can effect migrate freely over long distances and be absorbed at fixed sinks. The difference is that *fmd* is based on experimental data, and requires interpretation to extract a number, while *arcdpa* is based on the results of molecular dynamics (MD) simulations (most cases) (but also from order/disorder experiments) making it a more reproducible value. Because *arcdpa* does not take into account correlated recombination of nearby interstitial-vacancy pairs, its value is higher than that of the freely migrating defects. In most neutron irradiations of metals, recombination causes $\xi=1/3$, that is a third of the defects survive athermal recombination. The *fmd* represents the mobile fraction of the arc-dpa, which is about half.

Another measure of damage mentioned in the review by Nordlund et al. [16] is replacements per atom (rpa). Since interstitial-vacancy recombination is essentially random, many atoms return to the lattice at different positions than where they started. If all atoms are the same, this has no effect, but if, for example, there is a solid solution of Cr in Fe, the Cr atoms may undergo “diffusion” by this atomic replacement process. If the replacements occur in intermetallic ordered compounds, the replacement the creation of antisite defects contributes to chemical disordering and amorphization. Because of its

nature the rpa can also be obtained from order/disorder experiments. The actual ratio of rpa per dpa depends on the T_{dam} (nuclear damage energy) and has been calculated at about 5 for 100 eV and about 20 for 10 keV in three different metals.

Which damage parameter to use in studying a particular macroscopic radiation effect of interest depends on the mechanism of damage accumulation. For example, single, mobile defects are very important in irradiation creep and void swelling, and thus arcdpa or fmd would be an appropriate gauge, while hardening may be governed by the formation of defect clusters in the cascade which correlate more directly with dpa, and disordering and amorphization may correlate more directly with rpa.

12.8 Other Displacement Mechanisms

Although fast neutron elastic scattering is the main contributor to radiation damage other displacements processes can also contribute, the main ones being (i) gamma-induced displacements, (ii) thermal-neutron reactions and (iii) inelastic scattering.

12.8.1. Gamma Displacement damage

Gamma rays do not deliver energy directly to atomic nuclei³. Rather, electrons are energized by one of three possible interactions of the gamma ray with electrons of the solid: the *photoelectric effect*, *Compton scattering*, and *pair production*. These processes are each dominant at different energy ranges, but in all cases the net effect is to produce energetic electrons, which, in turn, can cause displacement damage to the solid.

Compton scattering is by far the most important of these interactions. The Compton effect, as the interaction is called, describes an elastic collision between a gamma ray and a free electron initially at rest. Figure 12.18 diagrams the energy partitioning in the collision.

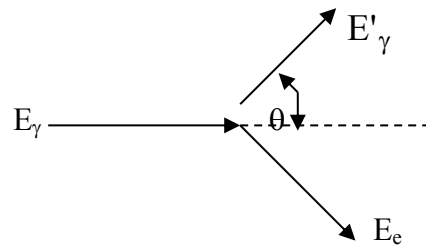


Fig. 12.18: The Compton Effect

Conservation of energy gives:

$$E_\gamma = E'_\gamma + E_e \quad (12.84)$$

³ In principle it is possible for (γ, p) or (γ, n) reactions to cause damage from the creation of an energetic particle, but its cross sections are low.

Which, together with the momentum conservation equation, yields the *Compton Formula* [17] for the energy of the scattered gamma ray:

$$E'_\gamma = \frac{E_\gamma m_e c^2}{m_e c^2 + E_\gamma (1 - \cos \theta)} \quad (12.85)$$

where $m_e c^2 = 0.51$ MeV is the rest energy of the electron

The differential scattering cross section (per electron) is given by the *Klein-Nishina Formula* [17]:

$$\sigma_s(E_\gamma, E'_\gamma) = \frac{0.15}{A^2 N_{Av}} \frac{m_e c^2}{E_\gamma E'_\gamma} \left[1 + \left(\frac{E'_\gamma}{E_\gamma} \right)^2 - \left(\frac{E'_\gamma}{E_\gamma} \right) \sin^2 \theta \right] \quad (12.86)$$

where A is the mass number of the atoms of the solid and N_{Av} is Avogadro's number.

The $\sin^2 \theta$ term can be expressed in terms of E'_γ by use of Eq (12.85). The range of E'_γ over which Eq (12.86) applies is obtained from Eq (12.85) by setting

$\theta = 0$ ($(E'_\gamma)_{\max} = E_\gamma$) and

$\theta = \pi$ ($(E'_\gamma)_{\min} = \frac{1}{2} m_e c^2$ if $E_\gamma \gg 0.255$ MeV)

For calculating the damage due to the Compton electrons, we need the differential cross section in terms of the electron energy, not the energy of the scattered gamma ray. These two differential cross sections are related by:

$$\sigma_s(E_\gamma, E_e) dE_e = \sigma_s(E_\gamma, E'_\gamma) dE'_\gamma$$

or

$$\sigma_s(E_\gamma, E_e) = \sigma_s(E_\gamma, E'_\gamma) \left| \frac{dE'_\gamma}{dE_e} \right| = \sigma_s(E_\gamma, E_\gamma - E_e) \quad (12.87)$$

The last equality results from taking the differential of Eq (12.84) and using the same equation to eliminate E'_γ . Therefore, $\sigma_s(E_\gamma, E_e)$ is obtained by replacing E'_γ by $E_\gamma - E_e$ in Eq (12.86) and on the left hand side of Eq (12.85) and eliminating θ between these two equations.

From the analog of the neutron case, the displacement cross section for a photon of energy E_γ can now be calculated for the electron produced by Compton scattering (Eq (12.60)) and weighting the probability of a Compton electron with the Klein-Nishina formula (Eq (12.72)) converted to electron energy by Eq (12.73):

$$\sigma_d(E_\gamma) = \int_{E_d/\Lambda}^{E_\gamma} \frac{\sigma_s(E_\gamma, E_e)}{\sigma_s(E_\gamma)} dE_e \int_{E_d}^{\Lambda E_e} \sigma_s(E_e, E) \nu(E) dE \quad (12.88)$$

where from Eq (12.10) with $M_1 = m_e$ and $M_2 = A$, the mass number of the atoms in the solid, $\Lambda = 2.2 \times 10^{-3}/A$. Sufficient energy transfer to cause a displacement in iron, for example, requires $E_e \geq 0.65$ MeV, assuming a displacement threshold $E_d = 25$ eV.

The total Compton scattering cross section for a gamma ray of energy E_γ is:

$$\sigma_s(E_\gamma) = \int_{\frac{1}{2}m_e c^2}^{E_\gamma} \sigma_s(E_\gamma, E_e) dE_e \quad (12.89)$$

Electron–atom scattering can be assumed to be isotropic in the center-of-mass system, so the differential energy-transfer cross section is the electron analog of Eq (12.71) for neutrons:

$$\sigma_s(E_e, E) = \frac{\sigma_s(E_e)}{\Lambda E_e} \quad (12.90)$$

where $\sigma_s(E_e)$ is the total scattering cross section for electrons and lattice atoms. To cause one or more displacements, the electron must interact with the bare nuclei of the atoms. The interaction for this process is purely Coulombic, so the cross section is given by the Rutherford formula.

Figure 12.19 shows the displacement cross sections calculated for Fe for all three sources of energetic electrons. It is clear that the dominant component is Compton scattering.

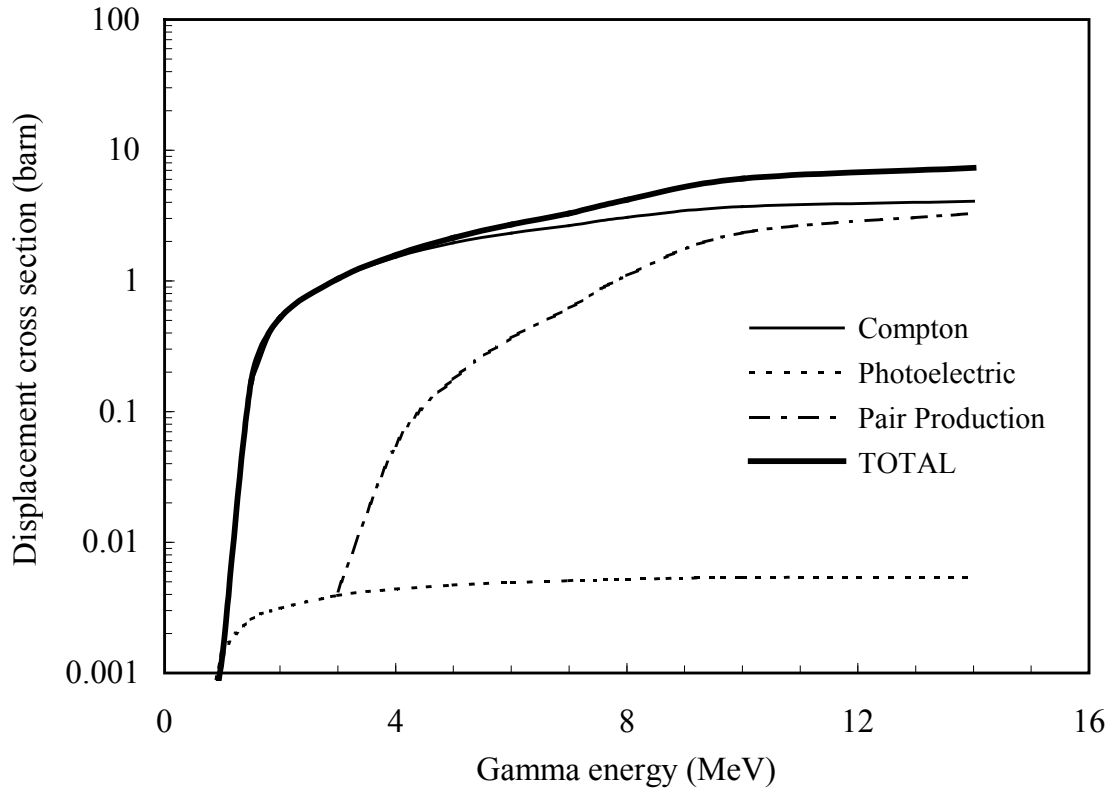


Fig. 12.19 Gamma displacement cross section as a function of gamma energy in iron [18]

Finally, the dpa rate due to a specified photon spectrum $\phi(E_\gamma)$ is, by analogy to Eq (12.69) neutrons, given by:

$$k_\gamma = \int_{E_{\gamma \min}}^{\infty} \sigma_d(E_\gamma) \phi(E_\gamma) dE_\gamma \quad (12.91)$$

where $E_{\gamma \min}$ is the photon energy that will just deliver energy E_e/Λ to the struck electron, which in turn is just capable of imparting E_d to a lattice atom. Eliminating E'_γ between Eqs (12.84) and (12.85), $E_{\gamma \min}$ is:

$$\frac{E_{\gamma \min}}{m_e c^2} = \frac{1}{2} B \left(\sqrt{1 + 2/B} + 1 \right) \quad (12.92)$$

where

$$B = \frac{E_d / \Lambda}{m_e c^2} \quad (12.93)$$

If B were very large (which it is not), the result would be $E_{\gamma\min} = E_d/\Lambda$. For iron, $B = 1.28$, and Eq. (12.78) gives $E_{\gamma\min} = 0.85$ MeV.

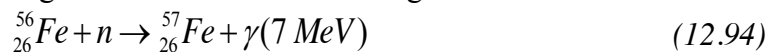
Inside a reactor core, and in most cases for the pressure vessels too, the displacement rate caused by the gamma flux arising from both fission products and activation products decaying to their stable species is much smaller than the neutron elastic collision displacement rate (typically < 1%). In a few cases, however, especially when a large water gap exists between the core and the pressure vessel to thermalize the fast neutrons leaking from the core, k_γ can be of the same order of magnitude as k_n . One well-known case relates to the accelerated embrittlement observed in the HFIR (High Flux Isotope Reactor) at Oak Ridge in the early 1990s [19]. The measured levels of embrittlement at the pressure vessel were found to be higher than expected for the levels of damage calculated by the NRT model (which considers only neutron damage). It was then realized that because of the large water gap, the gamma displacements were comparable to the neutron displacements. Taking the gamma displacements from Eq (12.91) into account removed the apparent discrepancy. Gamma induced displacement damage is also important in situations where not only the total amount of damage but also the damage structure (in particular the freely-migrating defect fraction) is important to evaluating the effects of irradiation. This will be discussed in more detail in the following section and in the next chapter.

12.8.2. Thermal Neutron Reactions

Thermal neutron reactions can also cause damage to reactor components. Having absorbed a thermal neutron, a nucleus undergoes radioactive decay, typically emitting an energetic gamma or alpha particle. The emitted particle can cause damage. By conservation of momentum, the decaying atom recoils in the opposite direction, often with an energy sufficient to cause further displacements. The specific reaction depends on the atoms present, but several reactions are possible, including (n,α), (n,γ), (n,n'), (n,p), etc. One example, for gamma decay in Fe, is shown below.

Example # 5 displacements due to neutron activation of iron

Iron can be activated by absorbing a thermal neutron according to



By conservation of momentum $P_\gamma = \frac{E_\gamma}{c} = P_{Fe}$ and the energy of the recoil nucleus is

$E_{Fe} = \frac{P_{Fe}^2}{2M}$, which is 460 eV, enough to cause 9 displacements according to Eq (12.57) if $E_d=25$ eV.

We can estimate that for a thermal neutron flux of $10^{13} \text{ n.cm}^{-2}.\text{s}^{-1}$, and a thermal cross-section for the (n,γ) reaction in iron equal to 3 barns, the displacement rate would be $2.7 \times 10^{-8} \text{ dpa/s}$, which is quite a bit lower than the displacement rate by elastic collisions with fast neutrons. Note that the displacements caused by the 7 MeV photon would also have to be considered here.

12.8.3 Inelastic Scattering

Inelastic scattering involves forming a compound nucleus by absorption of a fast neutron by the nucleus of an atom and subsequent emission of a neutron of lower energy. This reaction is called *inelastic scattering* or (n,n') . It only occurs above a certain threshold energy of the incident neutron, which for typical metals is above 1 MeV. Because the fission spectrum contains a considerable fraction of neutrons of energy above 1 MeV, the (n,n') reaction is a significant damage mechanism.

The threshold neutron energy for inelastic scattering for an atom mass M is

$$E_n^{th} = \frac{M+1}{M} E_{ex} \quad (12.95)$$

where E_{ex} is the excitation energy, or the energy level above the ground state that is populated by the collision with the incident fast neutron. That the threshold energy is greater than the excitation energy is a consequence of momentum conservation.

The analog of Eq (12.9) for inelastic scattering is

$$E = \frac{1}{2} \Lambda E_n \left[1 - \frac{1}{2} \frac{E_n^{th}}{E_n} \left(1 - \frac{E_n^{th}}{E_n} \right)^{1/2} \cos \theta \right] \quad (12.96)$$

The maximum energy transferred corresponds to $\cos \theta = -1$ and the minimum to $\cos \theta = 1$, so the analog of Eq (12.11) is

$$E_{\max,\min} = \frac{\Lambda E_n^{th}}{2} \left[\alpha \left(1 - \frac{1}{2\alpha} \pm \sqrt{1 - \frac{1}{\alpha}} \right) \right] \quad (12.97)$$

where $\alpha = \frac{E_n^{th}}{E_{ex}}$. Since inelastic scattering involves the formation of a compound nucleus, the emitted neutron is isotropic in the CM. The analog of Eq (12.71) is

$$\sigma_n^{in}(E_n, E) = \frac{\sigma_n^{in}(E_n)}{\Lambda E_n \sqrt{1 - \frac{E_n^{th}}{E_n}}} \quad (12.98)$$

and the displacement cross section for inelastic scattering is

$$\sigma_d^{in}(E_n) = \frac{\sigma_n^{in}(E_n)}{\Lambda E_n \sqrt{1 - \frac{E_n^{th}}{E_n}}} \int_{E_{min}}^{E_{max}} v(E) dE \quad (12.99)$$

Example # 6 Displacements from inelastic scattering of neutrons from iron

The inelastic scattering induced displacements become important above 1 MeV neutron energy. Ref [20] calculates the inelastic displacement cross-section at about 500 barns and at 2200 barns at 10 MeV. Assuming a monoenergetic flux of $10^{13} \text{ n.cm}^{-2}\text{s}^{-1}$ at these energies would give respectively displacements rates of $5 \times 10^{-9} \text{ dpa/s}$ and $2.2 \times 10^{-8} \text{ dpa/s}$.

12.9. Charged-particle irradiation

For the sake of completeness, charged-particle irradiation (electrons and ions) generated by accelerators is discussed in this section. The motivations for using charged particle irradiation in experimental radiation damage studies are, first, that the ion irradiation displacement rates are orders of magnitude higher than those achievable under neutron irradiation, so equivalent doses (in dpa) are attained in hours instead of years; second the effects of experimental variables such as temperature and dose rate can be explored with greater ease; and third, ion or electron irradiated samples are less radioactive than samples irradiated with neutrons, making them easier to handle. The disadvantage of accelerator-produced particle irradiation is that the depth of damage is localized to at the most within a few tens of microns of the surface.

In general, the results obtained in such experiments do not have a one-to-one correspondence with results of neutron irradiation. Nor should such a close correspondence be expected, as the irradiations are quite different, in particular, ion irradiation has a much higher dose rate, and often has to be run at higher temperatures to obtain equivalent microstructures [21, 22]. Table 12.2 shows the differences between the different types of irradiation for typical values of irradiation parameters in reactors, accelerators and electron microscopes.

Table 12.2 Comparison of neutron, ion and electron irradiation in metals. For ion and electron irradiation, typical fluxes in accelerators and high energy electron microscopes (when the beam is condensed) are given

	Fast Neutron	Ion	Electron
Typical Flux (particle.cm ⁻² .s ⁻¹)	5×10^{13} (LWR core)	10^{11} - 10^{12} (Ion accelerator)	5×10^{19} (High Voltage Electron Microscope)

Displacement Rate (dpa/s)	10^{-7}	10^{-4} - 10^{-5}	10^{-2} - 10^{-3}
Irradiation time to 1 dpa	~ 4 months	4 to 40 h	2-20 minutes
Temperature	Reactor temperature (coolant ~ 300 °C)	adjustable	adjustable
Macroscopic gradients of damage	Small gradient; follows neutron flux attenuation	Sharp nuclear stopping peak at the end of ion range	Homogeneous in thin foil, but sharp lateral gradients (beam spot)
Sample Volume Irradiated	Bulk (homogeneous over large volumes, whole components irradiated)	Near surface (on the order of 1-10 μm for typical irradiations, laterally ~ 1cm ²)	Thin Foil (100 nm thick, beam is about 1 μm^2)
Microscopic Spatial distribution of damage	Inhomogeneous (dense cascades present)	Inhomogeneous (variable density cascades)	Homogeneous (mostly isolated Frenkel pairs)
Freely Migrating Defect Production (% of NRT value)	1-5	~10-50	~ 100

12.9.1 Electron Irradiation

Energetic electrons include Compton electrons, beta particles from nuclear disintegrations and electrons produced by an accelerator. These electrons create atomic displacements by direct scattering from atomic nuclei. Electron irradiation differs from neutron and ion irradiation in two ways: (i) even for electron energies in the MeV range the energy of the PKA created by an electron atom collision is not much greater than the displacement energy, making displacement cascades rare and (ii) the electron velocities are high enough to require relativistic treatment of collision dynamics. Instead of the classical result (Eq. (12.11)), the maximum energy transferred to a nucleus struck by an electron is given by

$$E_{\max} = \frac{1}{2} \left(\frac{E_e}{m_e c^2} + 2 \right) \Lambda E_e \quad (12.100)$$

instead of the classical result $E_{\max} = \Lambda E_e$ used in the upper limit of the integral in Eq (12.88). The minimum electron energy to cause displacements is arrived at by setting $E_{\max} = E_d$ in Eq (12.100) and rearranging

$$E_{e\min} = m_e c^2 \left[-1 + \sqrt{1 + \frac{2E_d / \Lambda}{m_e c^2}} \right] \quad (12.101)$$

If the second term in the square root is small compared to unity (that is if the energy is small compared to relativistic energies), a Taylor series expansion gives the classical result $E_{e\min} = E_d / \Lambda$.

12.9.2. Ion Irradiation

The principal difference between irradiation with ions and neutrons is that the former interacts with atoms with a cross section on the order of 10^{-16} cm^2 , whereas typical neutron –nucleus cross sections are on the order of 10^{-24} cm^2 . The result is that ions lose their energy much faster than neutrons do as they transverse a solid. This difference causes both a higher displacement rate due to ion interactions and a spatial gradient of damage as the displacement cross section increases sharply with decreasing ion energy. Since irradiation effects depend on the balance between irradiation damage and thermal annealing, increasing the displacement rate affects phenomena such as, for example, the peak void swelling temperature. In Chapter 22, we show that this temperature is higher under ion irradiation than under neutron irradiation.

Ion irradiation illustrates all the interactions of radiation with solids that were presented earlier in this chapter. In particular, the regions of electron stopping and nuclear stopping are illustrated in Fig. 12.20 (a), which is a TEM micrograph of a cross-section of MgAl_2O_4 (spinel) irradiated with 2 MeV Al^+ ions at 650°C to a level of 14.1 dpa. The contrast observed is the formation of dislocation loops which are more numerous in the nuclear stopping region, as seen from a TRIM simulation.

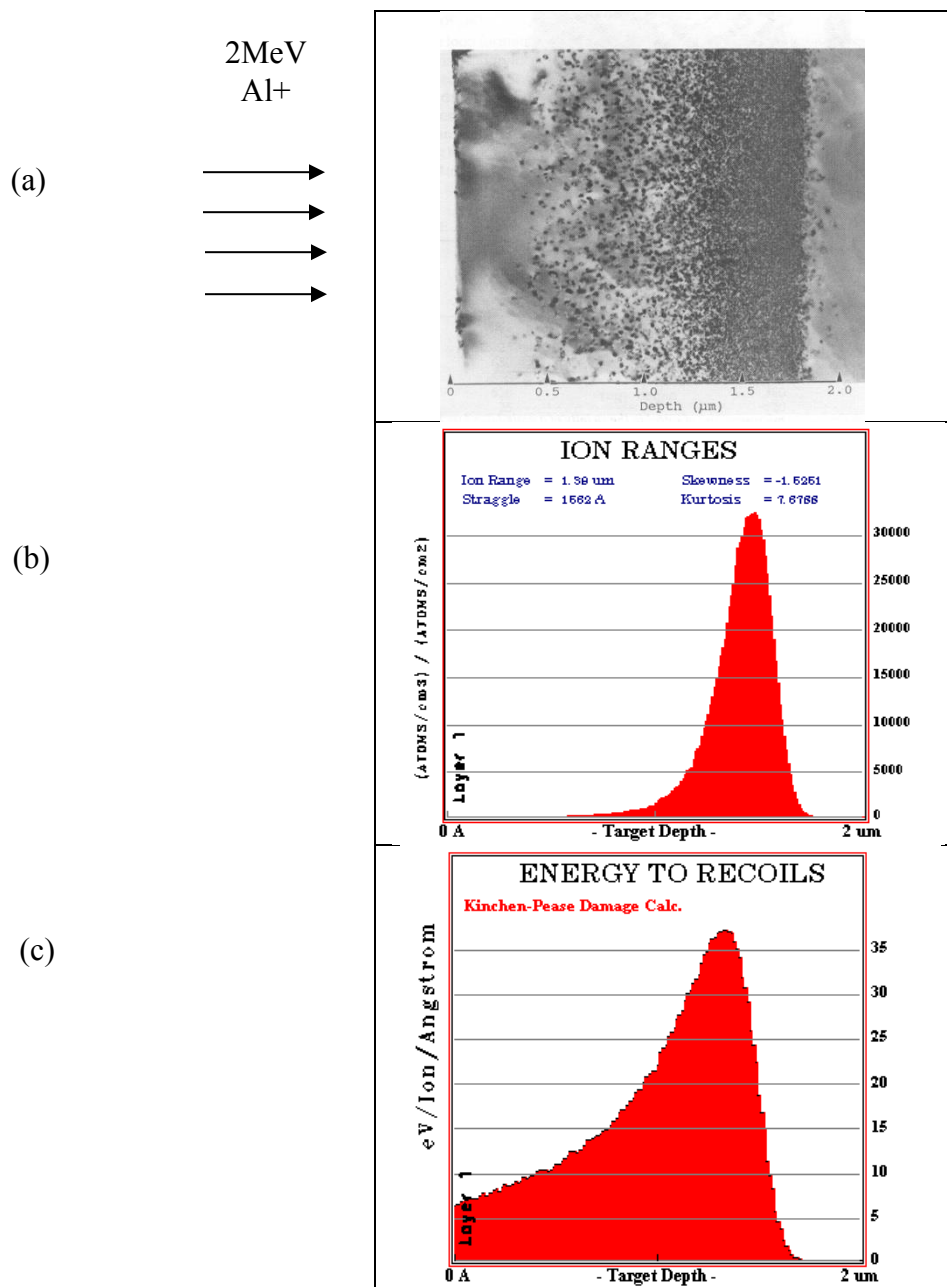


Figure 12.20 (a) TEM bright field image showing the variation of displacements damage with depth during 2 MeV Al⁺ ion irradiation of MgAl₂O₄ (spinel) [23]. (b) Plot of implanted ion distribution and (c) Displacement damage as a function of distance. Both simulations simulation performed using SRIM[6]. The displacement energy was 40 eV for all atoms and the K-P approximation was used.

The energetic particles penetrate the solid from the left. At the beginning they interact mostly with electrons, causing very few displacements. After a distance of about 0.5-1 microns, (corresponding to a decrease of ion (PKA) energy down to the limit between nuclear and electronic regimes), the ion starts interacting with nuclei. This is seen in the

center of Fig. 12.20(c) where the displacement rate increases abruptly, thereby generating a high defect concentration. At the end of the displacement region, the ion comes to rest as a neutral atom (Fig.12.20 (b)).

12.9.3 TRIM and SRIM codes

The TRIM (Transport of Ions in Matter) and SRIM (Stopping and Range of Ions in Matter) codes calculate the interactions of energetic ions with the atoms in solids. Since its inception, due to its ease of use and sound physical basis, it has become the standard method of calculating dpa and range of ions in matter. The program runs a simulation of many histories, during which the probabilities of nuclear and electronic collisions are weighed according to their probabilities, as discussed below. The program does not consider nuclear reactions, the crystal structure of the material (materials is disordered (or non-crystalline) with a specified density) or the accumulation of damage (each ion sees virgin material). The program does explicitly account for polyatomic targets, atomic sputtering, and allows for up to three layers of material with up to four elements in each. The importance of atomic sputtering can also be directly evaluated. No thermal spikes are considered.

The inputs are the incident atom, its energy and angle of incidence, target thickness, density and composition, displacement energy for each atom in the solid, and the surface energy. The user may choose a detailed calculation with full damage cascades or a K-P based approximation, which takes the primary recoils and calculate the number of displacements using equation (12.57). Recently Stoller and others have shown that for recent versions of SRIM it is more accurate to use the latter option [24].

The program relies on the development of a universal interatomic potential which depends on ion energy, and the masses and atomic numbers of the atoms in question. The potential is of the form

$$V(r) = \frac{Z_1 Z_2 e^2}{r} \Phi\left(\frac{r}{a}\right) \quad (12.102)$$

where Z_1 and Z_2 are the atomic numbers of the energetic ion and the target atoms, e is the electron charge, r the interatomic distance and a is a screening length which depends on the atomic numbers of the two atoms by the semi-empirical formula:

$$a = \frac{0.8854 a_{Bohr}}{Z_1^{0.23} + Z_2^{0.23}} \quad (12.103)$$

where a_{Bohr} is the Bohr radius (the radius of the hydrogen atom, 0.53 Å). Φ is the “universal” screening function determined by fitting of the calculated interatomic potentials of 521 randomly selected element combinations given by:

$$\Phi\left[\frac{r}{a}\right] = \sum_{i=1}^4 A_i \exp\left[-B_i\left(\frac{r}{a}\right)\right] \quad (12.104)$$

The remarkable feature of Eq (12.104) is that it depends only on the atomic numbers Z_1 and Z_2 . It is very accurate for high energy collisions but does not accurately give the number of displacements for collisions less than a few tens of electron volts.

This empirical interatomic potential shown in Eq. (12.104) has been validated by extensive comparison to experiment. It has been implemented into a code that partitions the energy loss between electrons and nuclei. The procedure is to substitute Eq (12.88) into Eq (12.42) to find a relation between impact parameter and angle θ . At the beginning of each step, the code determines a “free flight” distance in the material equal to the target interatomic spacing at low energies and by a complicated function of the ion energy and scattering-atom density at high ion energies. At the end of the free-flight distance, the ion undergoes a nuclear collision with an atom at a randomly-selected impact parameter. The analog of Eq (12.51) for the universal potential determines the energy transferred to the PKA and the scattering angle. If the ion energy after the collision, $E'_i = E_i - E$, or the transferred energy E are lower than a specified displacement energy E_d , the calculation is terminated. If not, the program recalculates the free-flight distance for the two branches of the calculation (moving ion and struck atom) and the process continues until the energies of all atoms involved fall below E_d . The code keeps track of energy loss, number of displacements, ion range and various other parameters. The program has been validated by comparison to experiments and is available for free downloading at www.srim.org.

Example 12.7: dpa calculations from SRIM

Considering the plot shown in Fig. 12.20 (b), what is the maximum total displacement rate (dpa/s) observed in the spinel sample if the Al^+ ion flux is $100 \mu\text{A}/\text{cm}^2$? The density of spinel is $3.578 \text{ g}/\text{cm}^3$.

In the example given, atoms of Mg, Al, and O are displaced; we consider the sum of all displacements in this calculation. The plot in Fig.12.20 (b) shows a maximum value of approximately 0.2 displacements/ion.A.

The ion flux can be obtained by noting that $100 \mu\text{A}/\text{cm}^2$ is $10^{-3} \text{ Coulomb}/\text{s} \cdot \text{cm}^2$ which for single-charged Al is equivalent to $10^{-3}/1.6 \times 10^{-19}$ (ion/Coulomb), or a flux of $6.25 \times 10^{13} \text{ Al}^+/\text{cm}^2 \cdot \text{s}$.

In

We now note that in a 1 cm^2 irradiated area, in a 1 Angstrom slice (a volume of 10^{-8} cm^3), there is a mass of $3.578 \times 10^{-8} \text{ g}$. One mole of MgAl_2O_4 contains 6.023×10^{23} formula units and weighs 142 g. This slice thus contains 1.52×10^{14} formula units. Since the calculation does not follow the detailed cascades, it is not possible to partition the displacements among the different atoms. Assuming an equal probability of displacement for each atom, we have 1.06×10^{15} atoms in the slice. The value is then

0.2 disp/ion/A is equivalent to $0.2 / 1.06 \times 10^{15} = 1.88 \times 10^{-16}$ [displacements per atom/(ion/cm².s)], which multiplied by the ion flux gives a peak damage rate of 0.0118 dpa/s.

Problems

1. Two atoms of the same kind interact with an energy transfer cross-section given by

$$\sigma(E,T) = \frac{C}{\sqrt{ET}}$$

where C is a constant. What is the probability of scattering with a center of mass angle greater than 90 degrees?

2. The (n, α) reaction in ${}^{59}_{28}\text{Ni}$ releases a prompt α -particle of $E_{\alpha} = 4.8\text{MeV}$.

a) Using momentum conservation, calculate the recoil energy of the ${}^{57}_{26}\text{Fe}$ product nucleus.

b) Calculate the number of displaced atoms caused by the recoil according to the Kinchin-Pease and NRT models. Assume $E_d = 25\text{eV}$

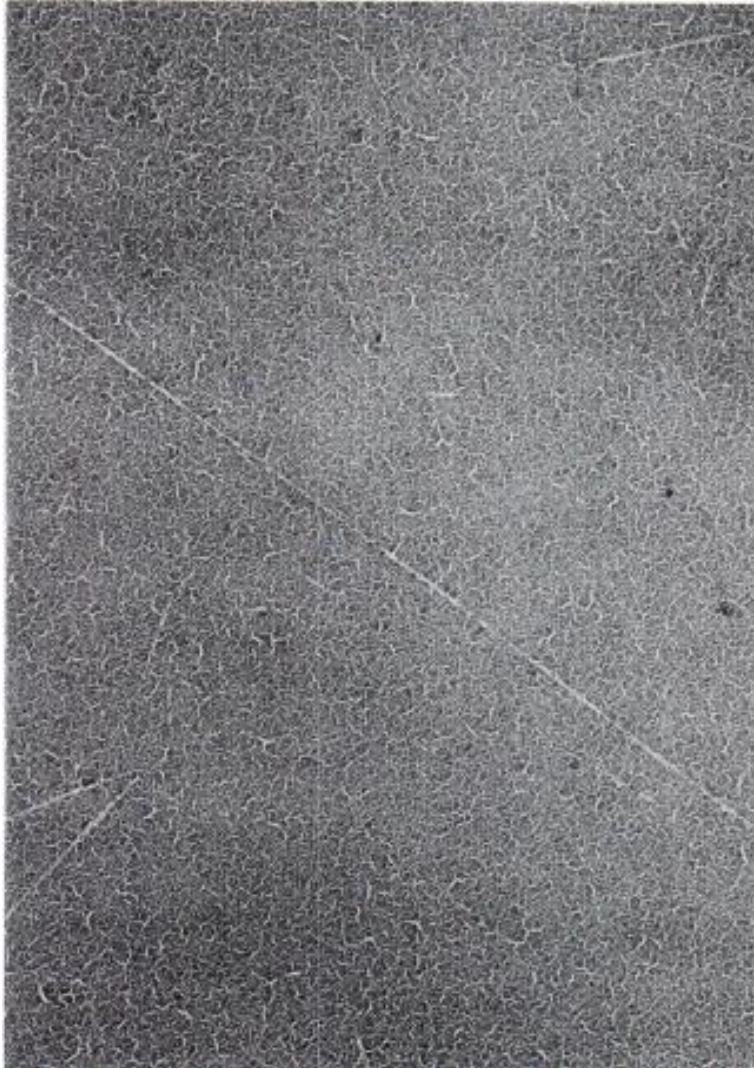
c) Using the K-P model, calculate the displacement rate (displacements/s.cm³) due to this mechanism, in a thermal flux of 10^{13} n/cm².s, if the density of iron is 7.8 g/cm³ and the thermal absorption cross section for Fe is 2.5 barns.

d) Compare this displacement rate to the displacement rate caused by fast neutrons for a fast flux of 10^{13} n/cm².s, ($\bar{E} = 1\text{MeV}$), also using KP. Assume elastic isotropic scattering and a scattering cross section of 3 b.

3. For a monenergetic fast neutron flux of energy 0.5 MeV calculate the number of displacements per atom in iron after a fast neutron fluence of 10^{22} n.cm⁻². Compare this calculation with that due to the displacements for a flux of 10 MeV neutrons. The displacement cross section for the 10 MeV neutrons is 3000 b.

4. An iron primary knock-on atom (PKA) is created with an energy of 100 KeV. According to the Kinchin-Pease model of displacement calculation and the Lindhard electronic stopping formula (eq. (12.23)), how far does the PKA travel before starting to interact with the nuclei in the solid?

5. The figure below shows a portion of a fission fragment track in UO₂. At one point the track changes direction indicating that the fragment has undergone a nuclear collision with an atom.



Assuming this is a $^{100}_{42}\text{Mo}$ fragment with a birth energy of 100 MeV, which has traveled 2 microns from where the fission took place to the place where it collides with the atom:

- a) What is the effective charge of the fragment at birth?
- b) Before the collision, the fragment loses energy by electronic excitation according to the Bethe formula. Calculate the energy at the point of the collision, assuming the mean excitation energy in the Bethe formula $\bar{I} = 8.8Z(\text{eV})$.
- c) If the scattering angle on the photograph is 5 degrees, calculate the energy transferred to the struck atom in the case of (1) an oxygen atom and (2) an uranium atom.

6. Calculate the average iron PKA energy in a fission neutron spectrum:

$$\phi(E_n) = A \times \exp(-E_n) \sinh(2E_n)^{1/2}$$

where E_n is the neutron energy in MeV. How does this value compare with the approximation of calculating the average PKA energy due to collision with the neutron of average energy? Assume isotropic, elastic scattering and an energy independent scattering cross section.

7. It is desired to evaluate the number of displacements per atom suffered by a piece of Zircaloy cladding oxide subjected to a neutron flux in a BWR. For the purposes of this calculation, assume the material is 66 at% Zr, and 33% O and that both atoms have a displacement energy of 25 eV. Use the neutron flux provided below, divided into 47 energy groups. Consider that the total oxygen scattering cross section is constant and equal to 3 barns. Assume isotropic scattering (the probability of generating a PKA of energy E is independent of E for the energy range considered). For Zr scattering, use Figure 12.17. The methodology to be utilized is the following:

- Each of these neutron energy groups will generate a distribution of energetic recoils of varying energy. Characterize each group by the total group flux at the average neutron energy in the group. Calculate the average recoil energy for each group.
- Using the KP formula, equation find the displacement cross section for each energy group.
- Multiply by the neutron flux per group to find the number of displacements per group and sum them over all energy groups to find the total number of displacements NRT for the material under consideration.

En (MeV) lower bound of group	BWR Core Shroud	Pressure Vessel Surface	En (MeV) lower bound of group	BWR Core Shroud	Pressure Vessel Surface
1.00E-11	7.61E+11	2.87E+08	3.69E-01	4.45E+10	4.26E+07
1.00E-07	1.07E+11	4.53E+07	4.98E-01	3.82E+10	3.43E+07
4.14E-07	3.50E+10	1.69E+07	6.08E-01	4.70E+10	4.27E+07
8.76E-07	3.66E+10	1.84E+07	7.43E-01	2.25E+10	1.73E+07
1.86E-06	5.03E+10	2.65E+07	8.21E-01	4.11E+10	3.37E+07
5.04E-06	3.85E+10	2.13E+07	1.00E+00	6.97E+10	5.58E+07
1.07E-05	6.46E+10	3.69E+07	1.35E+00	5.03E+10	3.58E+07
3.73E-05	5.16E+10	3.05E+07	1.65E+00	3.72E+10	2.62E+07
1.01E-04	3.83E+10	2.30E+07	1.92E+00	3.77E+10	2.62E+07
2.15E-04	3.76E+10	2.26E+07	2.23E+00	1.54E+10	1.03E+07
4.54E-04	6.18E+10	3.90E+07	2.35E+00	3.06E+09	2.05E+06
1.59E-03	3.96E+10	2.66E+07	2.37E+00	1.29E+10	8.38E+06
3.36E-03	4.05E+10	2.72E+07	2.47E+00	2.62E+10	1.77E+07
7.10E-03	3.62E+10	2.29E+07	2.73E+00	2.34E+10	1.68E+07
1.50E-02	1.74E+10	1.77E+07	3.01E+00	3.23E+10	2.55E+07
2.19E-02	6.19E+09	5.61E+06	3.68E+00	4.34E+10	4.12E+07
2.42E-02	7.97E+09	7.14E+06	4.97E+00	2.15E+10	2.95E+07
2.61E-02	1.04E+10	6.36E+06	6.07E+00	1.31E+10	2.49E+07
3.18E-02	1.32E+10	9.11E+06	7.41E+00	4.69E+09	1.13E+07
4.09E-02	3.19E+10	2.55E+07	8.61E+00	2.35E+09	7.40E+06
6.74E-02	3.93E+10	3.46E+07	1.00E+01	1.07E+09	4.15E+06
1.11E-01	4.86E+10	4.43E+07	1.22E+01	2.22E+08	1.28E+06

1.83E-01	5.46E+10	4.67E+07	1.42E+01	5.05E+07	3.10E+05
2.97E-01	3.42E+10	3.69E+07	1.73E+01		

8. It is desired to estimate the importance of considering polyatomic processes on displacement calculations in problem 12.7, and of considering KP and full damage cascade calculations. To do this use the TRIM code and compare it to the values calculated using the NRT model.

a) Choose two neutron groups and determine appropriate the maximum PKA energies E_1 and E_2 . Divide the energy interval between 0 and ΛE_{ni} and derive a set of PKA energies to run TRIM.

b) Run TRIM (using full damage cascades) for the set of PKA energies for the two pure elements. Obtain from TRIM in each case i) the number of oxygen displacements and, ii) the number of Zr displacements created by the set of PKA energies E , for all intervals between 0 and ΛE_{ni} .

c) Use the displacement values calculated to calculate a weighted displacement rate in the compound. Compare this value with the value obtained in problem 12.7 for the energy group in question.

d) Run TRIM for the compound material (2/3 O, 1/3 Zr). Compare the oxygen, zirconium, and total displacement rates obtained with those from part c). What are the differences?

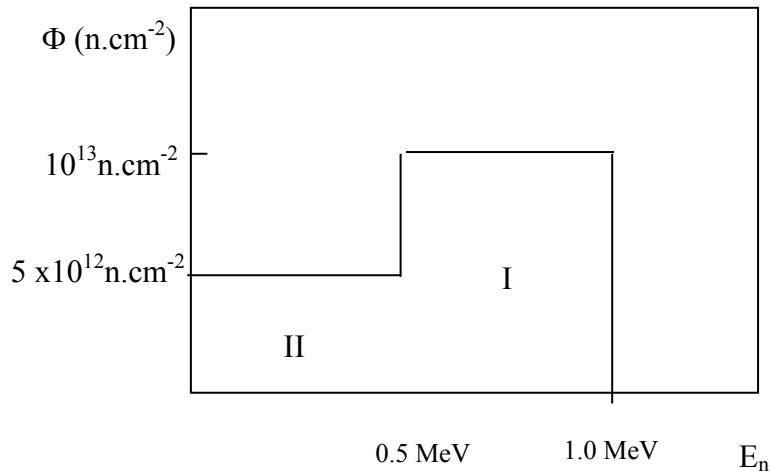
9. It is an experimental observation that during electron irradiation of a material below a given electron energy no displacements are possible, as predicted by equation(12.101). Occasionally it is possible to observe damage even below E_d as a result of secondary displacements through light element impurities. If bcc Fe has a displacement energy of 40 eV and contains C, calculate:

a) The minimum electron energy to cause displacements in pure Fe.

b) The minimum electron energy considering secondary displacements of the type electron \Rightarrow C \Rightarrow Fe. What is the maximum Fe recoil energy obtainable from 400 keV electrons through a secondary C displacement mechanism?

c) What purity Fe would be necessary to ensure that secondary displacements are limited to 1/100 of the primary displacements at an electron energy of 900 keV? The displacement cross-section for 900 keV electrons is 30 b in Fe and 20 b in C.

10. Given the following two-region neutron flux, incident on a Zr component, calculate the total displacement rate, from fast neutron collisions using the Kinchin Pease model



The displacement energy for Zr is 33 eV. See Fig.12.17 for the scattering cross section of neutrons in Zr.

- 11.** Redo the calculation in example 12.3, but taking into account the variation of the scattering cross section between 0 and 3 MeV, which you can approximate as a linear function.
- 12.** Calculate the distance of closest approach for two particles that meet head-on, and whose interaction is governed by the unscreened Coulomb potential (equation(12.46))
- 13.** A 40 eV atom of mass M_1 strikes a lattice atom of mass $M_2 = 2M_1$.
 - (a) What is the probability that the lattice atom is displaced?
 - (b) If the lattice atom is displaced, what happens to the other atom?
 Assume hard-sphere scattering and a displacement energy of 25 eV.

References

- [1] E. P. Wigner, *Journal of Applied Physics*, vol. 17, pp. 857-863, 1946.
- [2] C. Claeys and E. Simoen, *Radiation Effects in Advanced Semiconductor Materials and Devices*. Berlin: Springer, 2002.
- [3] A. Holmes-Siedle and L. Adams, *Handbook of radiation effects*, 1993.
- [4] M. T. Robinson, "Basic physics of radiation damage production," *Journal of Nuclear Materials*, vol. 216, pp. 1-28, 10// 1994.
- [5] D. R. Olander, *Fundamental Aspects of Nuclear Reactor Fuel Elements*: ERDA, 1976.
- [6] J. Ziegler, J. P. Biersack, and U. Littmark, *The Stopping and Range of Ions in Matter*. New York: Pergamon Press, 1985.
- [7] W. E. King, K. L. Merkle, and M. Meshii, "Determination of the threshold-energy surface for copper using in-situ electrical-resistivity measurements in the high-voltage electron microscope," *Physical Review*, vol. B 23, pp. 6319 - 6334, 1981.
- [8] P. Jung, "Atomic displacement functions of cubic metals," *Journal of Nuclear Materials*, vol. 117, pp. 70-77, 1983/7 1983.
- [9] ASTM, "Standard Practice for Neutron Radiation Damage Simulation by Charged-Particle Irradiation," American Society for Testing and Materials Standard Practice E521-96, 1996.
- [10] S. J. Zinkle and C. Kinoshita, "Defect production in ceramics," *Journal of Nuclear Materials*, vol. 251, pp. 200-217, 11/11/ 1997.
- [11] G. H. Kinchin and R. S. Pease, "The Displacement of Atoms in Solids," *Rep. Progress in Physics*, vol. 18, pp. 1-51, 1955.
- [12] M. J. Norgett, M. T. Robinson, and I. M. Torrens, "A Proposed Method for Calculating Displacement Dose Rates," *Nuclear Engineering and Design*, vol. 33, pp. 50-54, 1975.
- [13] D. M. Parkin and C. A. Coulter, "Total and Net Displacement Functions for Polyatomic Materials," *Journal of Nuclear Materials*, vol. 101, pp. 261-276, 1981.
- [14] "Evaluated Nuclear Data File VI (ENDF-VI)," Brookhaven National Laboratory 2006.
- [15] L. R. Greenwood and R. K. Smither, "SPECTER: Neutron Damage Calculations for Materials Irradiations," ANL/FPP/TM-197, 1985.
- [16] K. Nordlund, A. Meinander, F. Granberg, S. J. Zinkle, R. E. Stoller, R. S. Averback, *et al.*, "Primary Radiation Damage in Materials," OECD NEA2014.
- [17] R. D. Evans, *The Atomic Nucleus*: McGraw-Hill, 1955.
- [18] J. Kwon and A. T. Motta, "Gamma Displacement Cross Sections in Various Materials," *Annals of Nuclear Energy*, vol. 27, pp. 1627 -- 1642, 2000.
- [19] I. Remec, J. A. Wang, F. B. K. Kam, and K. Farrell, "Effects of Gamma-Induced Displacements on HFIR Pressure Vessel materials," *Journal of Nuclear Materials*, vol. 217, pp. 258-268, 1994.
- [20] D. G. Doran, *Irradiation Effects*, vol. 2, p. 249, 1970.
- [21] L. K. Mansur, "Theory of transitions in dose dependence of radiation effects in structural alloys," *Journal of Nuclear Materials*, vol. 206, pp. 306-323, 11/2/ 1993.
- [22] L. K. Mansur, "Void Swelling In Metals And Alloys Under Irradiation - Assessment Of Theory," *Nuclear Technology-Fusion*, vol. 40, p. 5, 1978.

- [23] S. J. Zinkle, "Dislocation Loop Formation in Ion Irradiated Spinel and Alumina," in *15th ASTM International Symposium on Radiation Effects on Materials*, Nashville, TN, 1992, STP 1125, pp. 749-763.
- [24] R. E. Stoller, M. B. Toloczko, G. S. Was, A. G. Certain, S. Dwaraknath, and F. A. Garner, "On the use of SRIM for computing radiation damage exposure," *Nuclear Instruments & Methods in Physics Research, Section B (Beam Interactions with Materials and Atoms)*, vol. 310, pp. 75-80, 2013.